TRABAJO FINAL DE MÁSTER

TÍTULO

DETERMINISTIC ASSESSMENT OF SLOPE FAILURE IN UNSATURATED VOLCANIC ASHES. THE CASE OF CERVINARA SLOPE

AUTOR

CLAUDIA JULIANA VILLARRAGA DIAZ

TUTOR

JEAN VAUNAT – FRANCESCA CASINI

ESPECIALIDAD

GEOTECHNICAL ENGINEERING

FECHA

MAY 2014

Dep. de Ingeniería del Terreno, Cartográfica y Geofísica
E.T.S. Ingenieros de Caminos, Canales y Puertos
UNIVERSIDAD POLITÉCNICA DE CATALUÑA

ABSTRACT

This thesis deals with the assessment of the failure mechanism of a shallow landslide triggered by rainfall in a slope of unsaturated volcanic ashes, located at Cervinara, Italy.

The region of Campania (Southern of Italy) had suffered in several occasions the consequences of this type of landslides. They have caused casualties, especially in the municipality of Cervinara. Additionally the quick growing of population in this region leads that to an increasing number of people exposed to a considerable risk.

For this reason, in the last years, research efforts have been made to define effective alarm system. But, in order to define adequately an alarm system is necessary that the failure mechanism of this landslides be completely understood.

This is why, in 2009 an instrumentation system was installed in a slope close to Cervinara to register the evolution of liquid pressure and water content within the slope. This monitoring system is still functional. Additionally a new test was developed in order to obtain information about the rainfall induced failure process. This test consists in a highly instrumented mock-up subjected to a specific rainfall intensity until failure

One of the sessions of the last Italian Workshop of landslides (October 2013) was dedicated to the hydrological modelling of landslides, through a benchmark exercise named Round Robin test. This exercise was focus in three analysis scales: laboratory test, mock-up test (flume test) and real case.

The benchmark considered two principal stages: back-analysis and prediction. For the back analysis phase the information provided consisted in different laboratory test, the characteristics and results of two different flume test, and the response of the monitoring station for the first seven months of 2011, as well as, the meteorological information for this months. Finally, the participants should simulate the response of an infiltration flume test with specific characteristics and the response to the real slope for an assigned record of precipitations and temperature.

To realized property this predictions, not just to define adequately the model (Geometry, boundary conditions and coupling) is important, The selection of the parameters that represent better the behaviour observed is crucial, in especial the hydraulic characteristics. Which are the most complex when dealing with unsaturated soils. In this thesis special attention is paid to the determination of the water retention curve.

Is important to mention that with predictions of failure time and the evolution of soil suction, of the flume test the modelling team was designated as winner of the benchmark on hydrological modelling of slopes at the Italian workshop on landslides, 23rd October 2013

RESUMEN.

Este trabajo se centra en el mecanismo de falla de los deslizamientos superficiales detonados por lluvias en un talud conformado por cenizas volcánicas inicialmente no saturadas, ubicado en Cervinara, Italia.

La región de Camapania (Sur de Italia) ha sufrido las consecuencias de este tipo de deslizamientos en varias ocasiones, generando en muchas muertes y daños a viviendas en especial en el municipio de Cervinara, además el rápido crecimiento de la población de esta zona, lleva a un importante incremento en el número de personas expuesto a un riesgo importante.

Es por esta razón que en los últimos años se han realizado importantes esfuerzos para definir sistemas de alarma que sean efectivos. Para definir adecuadamente un sistema de alarma es primordial conocer a fondo el mecanismo de falla de estos deslizamientos.

Por esta razón, desde el 2009 se viene monitoreando un talud cercano a Cervinara, en el cual se registra la evolución de los contenidos volumétricos de agua y presión de líquido en suelo, por otro lado, se ha desarrollado un ensayo laboratorio que busca obtener información específica sobre la falla de taludes debidos a lluvias, bajo condiciones delaboratorio, dicho ensayo consiste en un talud a escala que es instrumentado y sometido a una intensidad de lluvia especifica hasta que se produce la falla.

En el último *Italian Workshop of Landslides*, realizado en Octubre del 2013 una de las sesiones estuvo dedicada a la modelación hidrológica de deslizamientos, para lo cual se llevó a cabo una competición entre modeladores de diferentes universidades (*Benchmark*). Esta competencia se centró en tres escalas diferentes de análisis: ensayos de laboratorio, talud a escala y caso real.

El *benchmark* se dividió en dos fases: calibración y simulación, para la etapa de calibración la información presentada estaba conformada por: ensayos de laboratorio, características y respuesta de dos ensayos de infiltración sobre un talud a escala y la respuesta de la instrumentación del talud in situ para los primeros siete meses de 2011 así como la información meteorológica para estas fechas. Para la etapa de simulación se requirió calcular la respuesta para un determinado ensayo de infiltración y la respuesta del talud real para unas determinadas condiciones meteorológicas.

Para realizar exitosamente estas predicciones es importante definir adecuadamente las características de los modelos: geometría, condiciones de contorno y acoplamiento; pero aún más importante es definir adecuadamente los parámetros que mejor reproduzcan el comportamiento observado, en especial las características hidráulicas, ya que estas son las que representan mayor complejidad al tratarse de suelos no saturados. Para este trabajo final de master se ha tenido especial cuidado en la determinación de la curva de retención.

Es importante mencionar que con las predicciones realizadas para el talud a escala, el equipo de modelación fue seleccionado como ganador del ejercicio de *benchmark*, del tercer workshop de deslizamientos, octubre 23, 2013.

ACKNOWNLEDGMENTS.

I would like to express my gratitude to my tutor Jean Vaunat for his support, patient and explanations during the process of my master. Especially for his trust in my academic and working skills. I am grateful with Francesca Cassini because her support and guidance help me a lot to successfully complete my thesis.

I am very grateful to Jean Vaunat and Sebastian Olivella that trust in me and let me be part of the Code bright project. Which not only had helped me financially but has allowed me to learn a lot about numerical modelling, undoubtedly this learning had facilitated me the work realized for this thesis.

Finally, but very important, I would like to thank to my family especially to my parents and sisters because despite the distance they have always been there making me feel close to them. To my parents that always have been an inspiration and support during this process. And of course to Daniel because his important academic help but more important for his support and his emotional help that make easier this process.

NOTATION

A	Constant for liquid phase relative permeability
A_d	Dry albedo
A_l	Albedo
A_w	Wet albedo
b	Body forces
C_a	Specific heat of gas
D	Diffusion coefficient
d_s	Time span between sunrise and sunset
E_g	Specific internal energy of the gas
E_t	Evapotranspiration
E_s	Specific internal energy of the soil
E_v	Evaporation
f^a	Source/sink term of air
f^s	source/sink term of solid
f^w	source/sink term of water
H_c	Convected heat flux
h_{ao}	Free energy of air
h_{la}	Free energy of liquid water
h_v	Free energy of vapour
H_s	Sensible heat flux
H_r	Air relative humidity
i_c	Conductive heat flux
I_n	Index cloud
i_g^w	Diffusive flux of vapour
J	Square root of the second stress invariant of deviatoric stress
j_a	Flux of air
j_{EG}	Energy flux in the gas phase
j_{EL}	Energy flux in the liquid phase
j_{ES}	Energy flux in the solid phase
J_s	Advective flux of solid
J_{sr}	Surface runoff
J_w	Advective flux of water

j_g^a	Flux of air in gas phase
j_l^a	Flux of air in liquid phase
j_g^w	Flux of water in gas phase
j_l^w	Flux of water in liquid phase
K	Intrinsic permeability
k	Von Karman´s constant
LAI	Leaf area index
m	Parameter for the tortuosity
M_θ	Slope of critical state as a function of the lode angle
n	Parameter for the shape of the yield surface
P	precipitation
$\bar{p}$	Neat mean stress
P_{at}	Atmospheric pressure
P_c	Preconsolidation stress at specific saturation
P_g	Gas pressure
P_l	Liquid pressure
P_r	Reference mean stress (LC curve)
P_s	Tensile strength due to suction
P_c	Preconsolidation stress at saturated conditions
P_{0M}	Air entry value for macro - double porosity water retention curve
P_{0m}	Air entry value for micro - double porosity water retention curve
q_g	Gas flux
q_l	Liquid flux
R	Runoff
r	Parameter for the spacing ratio of the yield surface
R_a	Incident radiation of atmosphere to soil surface
r_a	Aerodynamic resistance
R_g	Incident solar radiation at the soil surface
R_{gl}	Maximum radiation at the soil surface
r_{lc}	Parameter to control infinite suction (LC curve)
R_n	Net radiation
R_s	Incident solar radiation
r_s	Leaf resistance

r_{smin}	Minimum surface resistance
r_{smax}	Maximum surface resistance
S_g	Gas saturation degree
S_l	Liquid saturation degree
S_{ls}	Maximum saturation degree
S_r	Soil radiation
S_{rl}	Residual saturation degree
s_l^a	Liquid saturation degree at anaerobiosis point
s_l^{fc}	Liquid saturation degree at field capacity
s_l^w	Liquid saturation degree at wilting point
T_a	Atmospheric temperature
t_m	Time at noon
T_0	Soil temperature
v_a	Wind velocity
veg	Vegetation fraction
w	Weight factor for micro - double porosity water retention curve
w_g^w	Vapour mass fraction
w_l^a	Air dissolved mass fraction
z_a	Screen height
z_0	Ground surface of roughness

GREEK SYMBOLS

β	Parameter to control stiffness (LC curve)
ε	Emissivity
ϕ	Porosity
γ	Empirical parameter for calculation of evapotranspiration
γ_g	Leakage coefficient
κ	Slope of unload/reload compression curve
κ_s	Parameter to account tensile strength due to suction
λ	Slope of the normal compression curve
λ_{dry}	Thermal conductivity of the dry porous media
λ_{sat}	Thermal conductivity of the saturated porous media

λ_M	Shape of water retention curve for macro
λ_m	Shape of water retention curve for micro
λ_{rp}	Power for liquid phase relative permeability
ρ_l	Liquid density
ρ_g	Gas density
ρ_{ga}	Atmospheric gas density
ρ_s	Solid density
ρ_v	Absolute humidity in the soil
ρ_{va}	Absolute humidity in the atmosphere
ρ_{vsat}	Saturated atmospheric absolute humidity
θ_a	Water content at anaerobiosis point
θ_{fc}	Water content at field capacity
θ_w	Water content at wilting point
θ_g^a	Apparent flux of air in gas phase
θ_g^w	Apparent flux of water in gas phase
θ_l^a	Apparent flux of air in liquid phase
θ_l^w	Apparent flux of water in liquid phase
σ	Stress tensor
τ_0	Parameter for the tortuosity
υ	Poisson ratio

TABLE OF CONTENTS

LIST OF FIGURES

LIST OF TABLES

CHAPTER 1
INTRODUCTION

Rainfall-induced landslides are very common natural hazards. According to Leroueil (2001) water within the slopes is the most common landslide triggering mechanism. This type of landslides occurred in zones where the material is under unsaturated conditions which contributes to the shear strength of the material.

The characteristics of water flow, liquid pressure variations and shear strength of the soils are the parameters that control the rainfall-induced slope failures. In fact the hydrological characteristics condition two principal aspects in the rain-induces landslides, determinate the occurrence of the landslide and defined the type of landslide triggered.

The infiltration process in the unsaturated soils is a very complex phenomena compare to the infiltration in saturated conditions because, the initial conditions defined by the profiles of liquid pressure and water content are not simple and depend on the antecedent hydrological history. Additionally, the capability of retaining water and the hydraulic conductivity of an unsaturated soil depend in the soil suction.

Usually, unsaturated soils present high values of matric suction which contributes to an additional shear strength. As the water infiltrates into the soil the matric suction reduces generating a decrease in the additional shear strength, causing the slope be more susceptible to failure. (Leroueil 2001; Rahardjo & Lee 2005; Rahardjo et al. 2011)

In general, all the studies realized in this field are directed to manage the risk of this type of landslides. Several empirical and physical models have been developed in order to obtain the rainfall conditions that initiate the event. In some cases is considered that the landslide is generated by a main rainfall event with a defined relation of intensity-duration in other cases is considered a combination of antecedent rainfalls. However, is not possible to achieve a universal relationship between intensity – duration of the rainfall before a landslide event. (Rianna et al. 2014; Springman & Askarinejad 2012)

In fact, Leroueil (2001) present several cases of landslides induced by rainfall with very different responses and triggering rainfall conditions. According to Springman & Askarinejad (2012) the key factors that affect the likelihood of a landslide are the location and origin of the slope. Which can be considered as constant in comparison with the other important parameters that control the environmental effects such as, meteorology, altitude, precipitations, vegetation and temperature.

The behaviour of the soil in the unsaturated zone of a slope (above the water table) is governed by the transfer of water and energy between the soil and the atmosphere boundary. Which is controlled by the infiltration characteristics of the soil and the precipitation, but also to the evaporation conditions, which is affected by the sun radiation, temperature and vegetation conditions. The vegetation plays an important role, on the one hand the canopy intercept part of the rainfall water and on the other hand the water uptake of the roots affect the flux conditions of water thought the soil (Blight 1997; Comegna et al. 2013)

The appropriated modelling of this relations, allows to obtain information about the evolution of the liquid pressure within the soil allowing to obtain the failure characteristics of the soil. For this thesis is used the finite element CODE_BRIGHT (Olivella et al. 1994) to developed

the modelling. The atmospheric boundary conditions is used with the aim to reproduce the atmospheric and vegetation conditions.

The principal natural hazard at which Campania (Southern of Italy) region is submitted are the shallow-landslides induced by rainfall. Every year this type of slides causes casualties and damage to houses and structures.

This region is covered by a shallow pyroclastic deposit with very high values of porosity (0.7 – 0.75) layer over a fractured limestone and with a steep slope inclination. The principal characteristic of the landslides occurred in this type of material is that present very weak warning signals of failure and long travel distance which makes them very dangerous.

For that reason important efforts are made to mitigate the risk of this slides but before a complete understanding of the failure mechanism is required. With this aim the site had been instrumented over the last years and additionally an infiltration laboratory test (flume test) was developed in order to evaluate the mechanism behaviour, considering just the rainfall effect. This test consist in a mock-up that is submitted to a specific rainfall intensity until the failure. (Olivares et al. 2009; Cascini et al. 2005; Damiano et al. 2012)

This thesis deals with the assessment of rain-induced landslides, considering different scales of study: flume test and real slope, considering the response observed in conventional laboratory tests. Is important to mention that the flume test consider a dense monitoring system allowing to capture the principal aspects of the failure observed.

This document is developed in five important chapters: Chapter 2 present the basic information available for the modelling exercise, considering the three scales of analysis the conventional laboratory test, the flume test and the real slope. The next section, Chapter 3 present the conceptual framework of analysis. In this chapter the thermo-hydro-mechanical coupling and the features of the atmospheric boundary condition are presented. Then, in Chapter 4 the numerical models are presented. Finally, Chapter 5 present the concluding remarks and future work.

CHAPTER 2
BENCH-MARK: ROUND ROBIN TEST

The region of Campania (Southern of Italy) is one of the most densely populated in Europe. This area had been subjected to a series of rainfall-induce flowslides which every year cause casualties an important damages to structures in this region. The fast population growth of this zone has generated an especial interest in the study of slope instability and early warning systems. The location of the zone is presented in Figure 2-1

This area is covered by an unsaturated pyroclastic soil considerate as stable due to the beneficial effect of suction on shear strength (apparent cohesion). But during the rainy season the rainfall infiltration causes the saturation of the soil reducing the apparent cohesion and generating the failure of the slope. In the last century 5 important events have occurred causing around 1000 casualties. One of the most important event occurred on December 16 of 1999 when a number of landslides were triggered in an area of almost 3.8 km^2 only a few kilometres from Cervinara town and after a precipitation of about 50 hours.

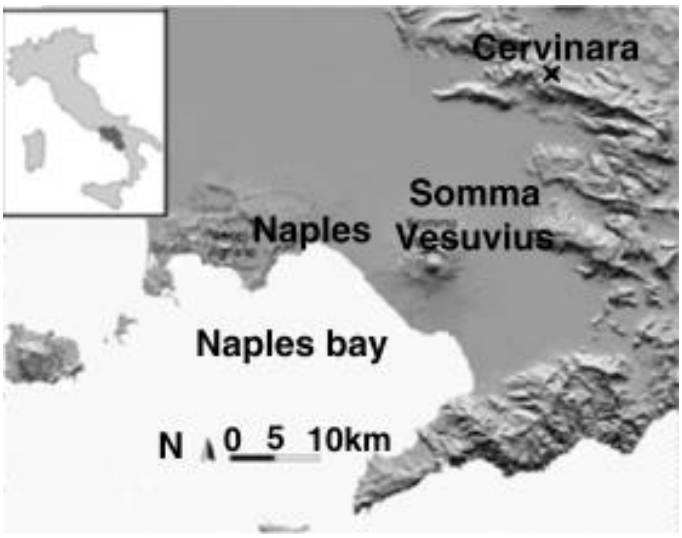

Figure 2-1 Cervinara slope location (Damiano et al. 2012)

In general this landslides have succeed in slopes with and inclination between 35º to 45º and a regular stratification constituted by a pyroclastic deposit composed by alternating ashes and highly vesciculated pumices layers of less than a few decimetres. The ashes layers may reach a few meters lying on a fractured limestone. The shallow failure is parallel to the limestone bedrock. (Olivares & Tommasi 2008; Damiano et al. 2012; Greco et al. 2010; Olivares et al. 2009)

One of the sessions of the third edition of the Italian workshop of landslides (3rd IWL) which took place between 23 and 24 of October 2013, was dedicated to a Round Robin test on landslides hydrological modelling. The Round Robin test basically consists in a competition among modellers based on a basic information at different scales of observation: small samples (laboratory test), infiltration flume test and the field.

The benchmark exercise was divided into two parts: the first part the modellers have to calibrate their models based on the data provided. In the second part the modellers were challenged to simulate:

- The response of a mock up flume test based just in the information of geometry, initial conditions and rainfall applied.
- The response of the real slope for a determined record of precipitations and temperature data.

2.1 BASIC INFORMATION

2.1.1 Small samples

In order to characterize the soil information of laboratory test over undisturbed and reconstituted specimens is given.

Water retention curve and hydraulic conductivity

To obtain the water retention curve 3 different types of test are presented: the transient test for infiltration and for evaporation (reconstituted sample), the pressure plate (reconstituted sample) and data obtained from suction controlled triaxial test (undisturbed sample). The data obtain are presented in Figure 2-2 suggest a bimodal water retention curve. As is expected for this type of soils characterized by the presence of itergranular and intragranular pores as was determinate in SEM observations realized in the pumices and ashes. (Olivares & Tommasi 2008)

The saturated hydraulic conductivity data were achieved with constant head test for saturated samples. Figure 2-3 present the relation between the hydraulic conductivity (m/s) with the mean normal stress. The mean value of saturated hydraulic conductivity is 1.44 e-6 m/s.

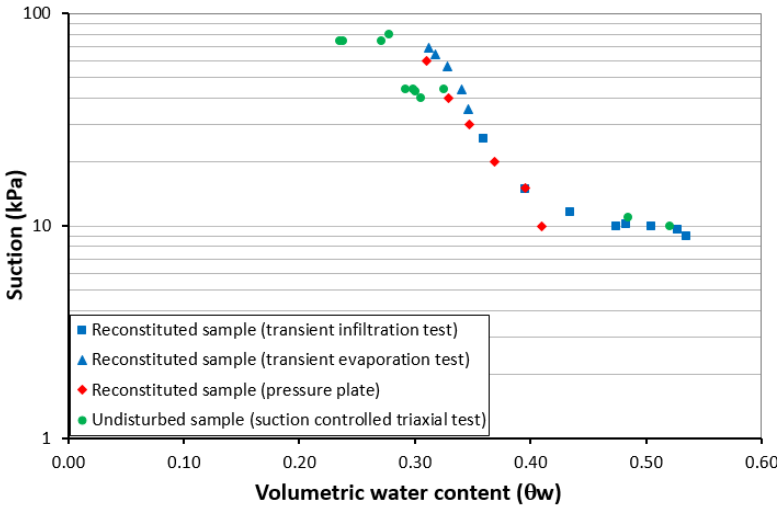

Figure 2-2 Water retention curve data

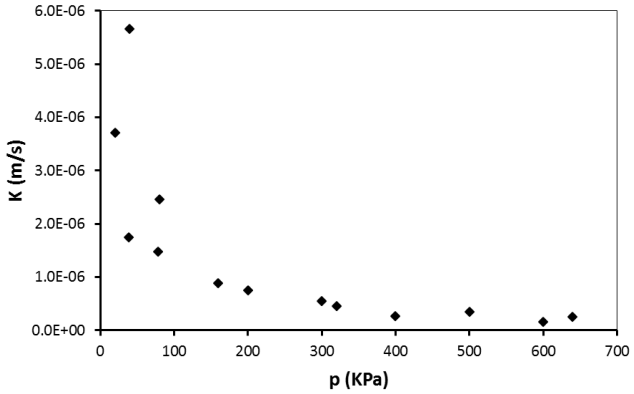

Figure 2-3 Saturated hydraulic conductivity

Compressibility and shear strength in unsaturated conditions.

Considering that the main goal of this exercise is the analysis of landslides triggered by rainfall in unsaturated soils. It is very important to have information of the compressibility of the soil and the shear strength both in saturated and unsaturated conditions.

Four compressibility test results had been presented one for saturated conditions and 3 for unsaturated conditions with a suction value of 40 kPa. Figure 2-4a present the results achieved. The results of the compressibility test can be related with the results of the hydraulic conductivity test allowing to relate the values of K with the void index (e). See Figure 2-4b.

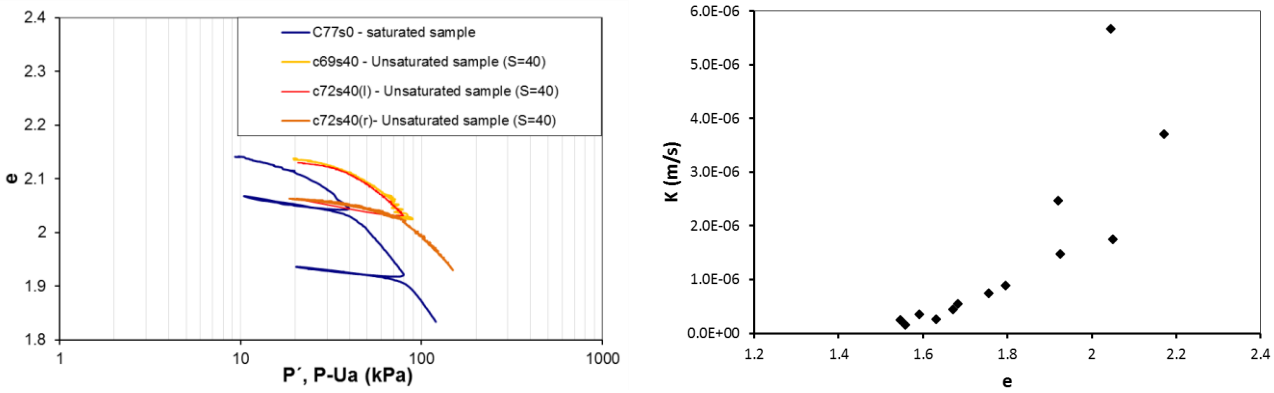

Figure 2-4 Compressibility test a) Compressibility test data. b) Relation between hydraulic conductivity and void ratio

On the other hand, the shear strength has been evaluated with triaxial test. Seven suction controlled triaxial test over undisturbed sampler were provided. The characteristics of all the test are summarized in Table 2-1 and Figure 2-5 present the response obtained.

Table 2-1 Suction control test characteristics

Sample	Suction (kPa)	Mean net stress (kPa)
C71USP	74	157
C70USP	74	89.3
C22USP	43	90
C4P1USP	44	60
C61USP1	44	23
C62USP1	74	22.4
1Cu1040	11	28.8

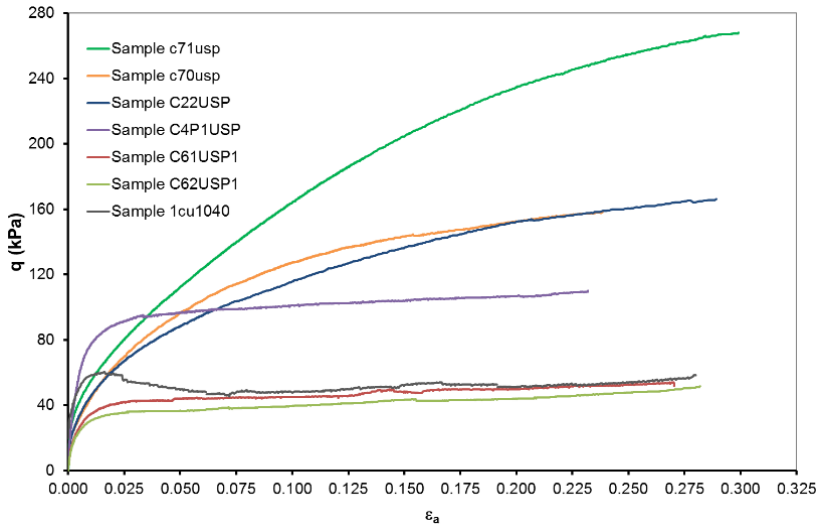

Figure 2-5 Triaxial test results

2.1.2 Flume test

The flume infiltration test is a mock-up test that allows to reproduce and investigate the rainfall induced landslide under a controlled environment. The infiltration flume test apparatus enable to considered different combinations of geometry and inclination. For this investigation the dimensions has been selected considering the assumption of infinite slope (ratio length/thickness less of 1/10).

In order to represent the characteristics of the actual slope the inclination considered is the 40º additionally the frictional contact between the soil and the limestone rock is simulated by calcareous grains glued at the bottom of flume and the sides of the flume are made of Plexiglas to simulate impervious boundaries. However, a geotextile drain is positioned at the foot of the slope to simulate a free flow boundary condition at this point. Figure 2-6 presents a sketch of the flume test equipment.

The rainfall is simulated by spray nozzles fixed parallel to the slope to reproduce vertical rainfall, the intensity of the rainfall is controlled to avoid erosion in the soil surface. To control the rainfall applied the rainfall intensity is measured by a horizontal tipping bucket rain gauge (RG in Figure 2-6) located at the foot of the slope. The infiltration test have been carried on with a constant value of rainfall intensity.

To evaluate the slope response the hydraulic and mechanical response are evaluated during the whole test. Considering four different measures:

- Soil matric suction: Measured by minitensiometers installed at different positions and depths within the slope (MT in Figure 2-6). For this experiment conventional jet-fill type tensiometers.
- Positive pore pressure: Carried out by miniature silicon diaphragm pressure transducer. This measures are realized at the bottom of the flume. (P in Figure 2-6)
- Soil water content profiles: Obtain by Time Domain Reflectometry (TDR) metallic probes. The profile of suction is obtain through the inverse profiling method proposed by Greco (2006) that allows to retrieve the moisture distribution along the TDR metallic probe buried in the soil, (TDR in Figure 2-6)
- Settlements: Monitored by laser sensors located at different zones of the slope with the optical axis perpendicular to the soil surface (LT in Figure 2-6). Based on the principle

of optical triangulation: a modulated light is projected on the soil surface and the distance is evaluated by the intensity of the reflected diffused light.

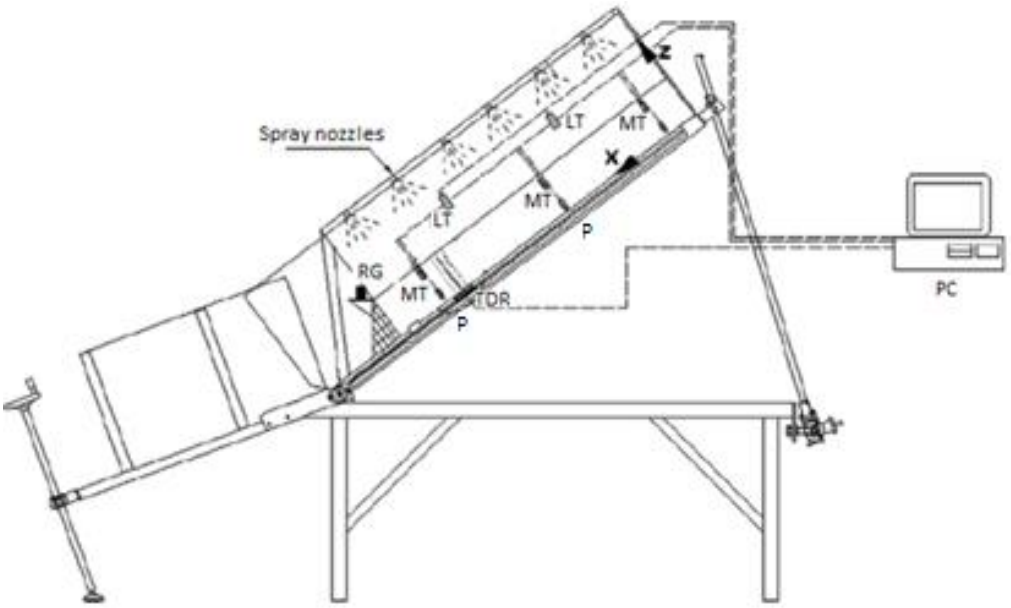

Figure 2-6 Flume test Sketch (Greco et al. 2010)

The pyroclastic deposit of the Cervinara slope is characterized by high values of porosity around 70% to 75%. To reach this values of porosity and guarantied its homogeneity the soil sample has been generated in layers of 0.5 cm and employing the moist tamping technique. The deposition of the soil have been made in the flume in horizontal position once the suction value is equalized the flume is tilted to the inclination desired. (Greco et al. 2010; Olivares & Tommasi 2008; Olivares & Damiano 2007; Picarelli & Vinale 2007; Olivares et al. 2009)

Two different infiltration experiments results has been presented (D3 and D4) both tests were carried on until the failure of the slide. The information offered consist in: geometry, rainfall intensity, and soil suction, settlements and liquid pressure records. The main characteristics of this tests are presented in Table 2-2

Table 2-2 Main Characteristics of infiltration test

Test	Soil Thickness (cm)	Slope Length (cm)	Initial Porosity n_0	Rainfall intensity (mm/h)	Initial mean suction (kPa)	Duration of the test (min)
D3	10	100	0.75	55	17.5	36
D4	10	120	0.76	56	43	30

Test D3

This test present an initial mean suction of 17.5 kPa. The slope has been subjected to a rainfall intensity of 55 mm/h for 36 minutes. In order to evaluate the behaviour of the test has been installed: 6 mini tensiometers, 5 laser sensors displacement transducers, 6 pore pressure transducers, one TDR probe and with the aim of controlling the rainfall intensity a rainfall gauge has been installed at the toe of the slope. The location of the monitoring system is presented in Figure 2-7.

Although a dense monitoring system has been installed, the results presented for this test are the recorded by: minitensiometers T3, T4 and T6; laser sensors L1 and L3; pore pressure transducer P1, P3 and P5, and the TDR probe. Test D3 results are shown in Figure 2-8.

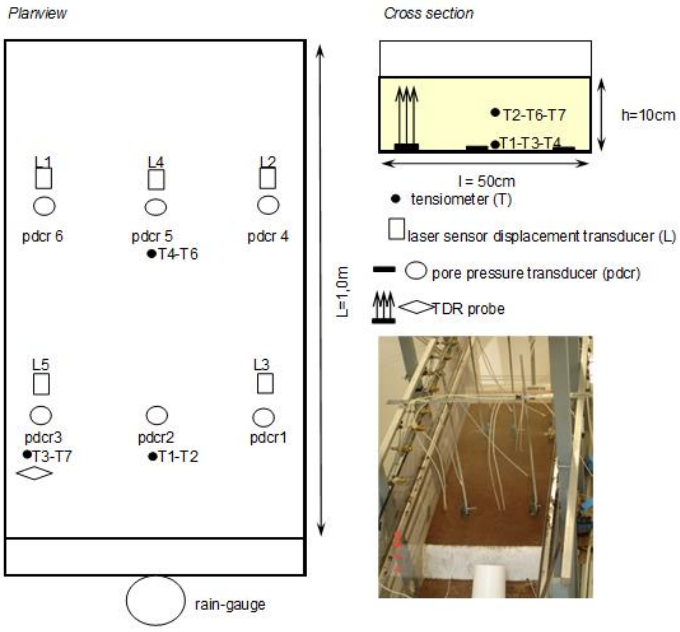

Figure 2-7 Test D3 monitoring system

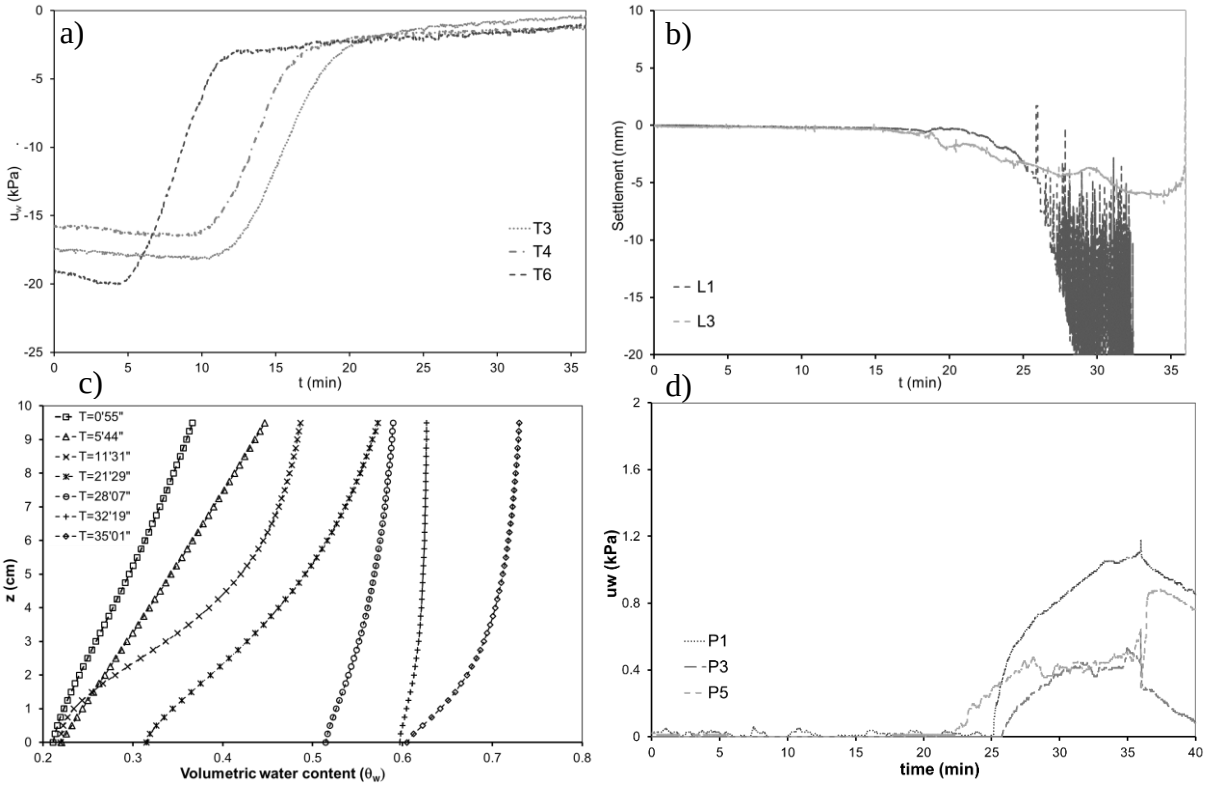

Figure 2-8 Test D3 results, a) Minitensiometers b) laser sensors settlements transducers c) volumetric water content profile d) pore pressure transducers.

Test D4

This test starts with a higher initial suction than test D3 43 kPa. The duration of this test is 30 minutes with a rainfall intensity of 56 mm/h. As in the case of test D3 the monitoring system installed is composed by: 5 mini tensiometers, 5 laser sensors displacement transducers, 6 pore pressure transducers, one TDR probe and the rainfall gauge. The location of the monitoring system is presented in Figure 2-9.

Just like the case of the test D3 not all the devices installed recorded appropriately the information. The evaluation of the test D4 has to be done based with the minitensiometers T2, T3, T4 and T6, the laser sensors L3 and L5 and the TDR probe, the Figure 2-10 present the response for the test D4

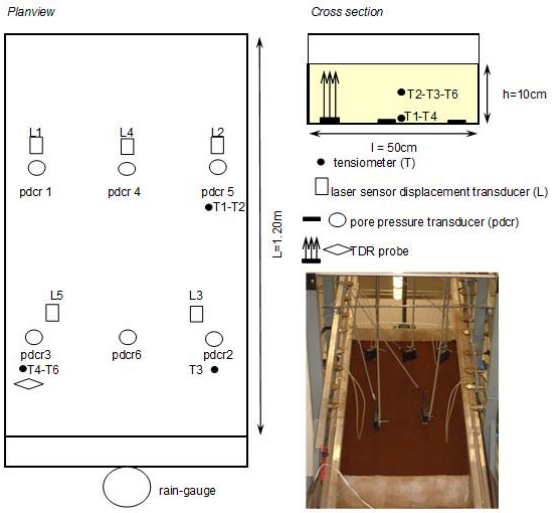

Figure 2-9 Test D4 monitoring system

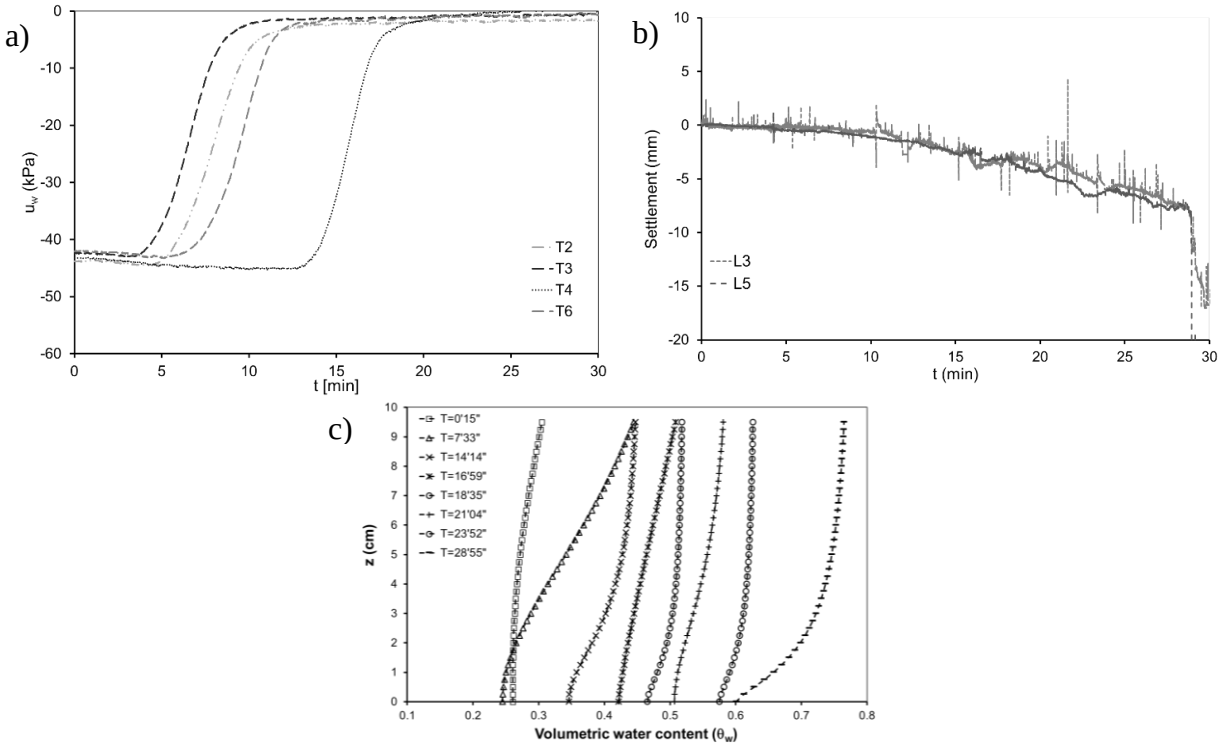

Figure 2-10 Test D4 results, a) Minitensiometers b) laser sensors settlements transducers c) volumetric water content profile

2.1.3 Field monitoring station

The site of study is located along the northeast slope of Mount Cornito near the town of Cervinara about 50km northwest of Naples, southern Italy. Close to the place were in 1999 a flowslide was triggered after a rainfall event of more than 24 hours.

The slope present an almost constant inclination of 40º with an elevation between 550m to 760m above the sea level. The pyroclastic deposit present a nearly continue thickness of 2.5 m. **¡Error! No se encuentra el origen de la referencia.** presents the typical layered soil cover. esides the slope is covered by woods mainly deciduous chestnuts (*Castanea sativa*) with few deciduous beeches (*Fagus sylvatica*) and also seasonal vegetation denser between May to September. Visual inspection show that roots present a maximum density in the first 0.4 m.

In August 2009 an automatically hydrological monitoring station was installed .Since then the capillarity tension and volumetric water content has been measured by standard jet tensiometers and time domain reflectometry (TDR) respectively. The measures are taken every two hour additionally a rainfall gauge with hourly acquisition was installed.

The instrumentation system consist in eight tensiometers and seven TDR metallic probes located at different depths between 0.6 and 1.6m grouped in two rows with 5 meters of separation. In addition some of the TDR probes are located close to the tensiometers in order to obtain a coupling between the volumetric water content and the capillarity tension. Figure 2-11 present a sketch of the monitoring system installed.

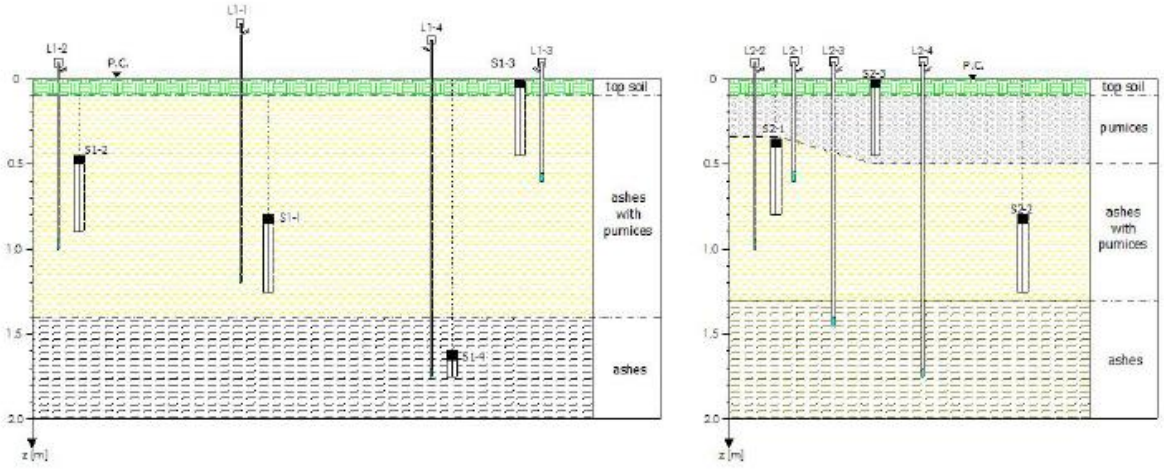

Figure 2-11 Typical stratigraphy and distribution of the field monitoring system.

Further, close to the place of study two meteorological stations are located: the Santa Maria a Vico station and the Pietrastonia station. In this meteorological station the data of temperature is recorded. The climate data for year 2001: temperature and rainfall are summarized in Figure 2-12.

Figure 2-13 present the matric suction and volumetric water content response at four depths from January 1 of 2001 to July 27th 2001. This data can be compared with the rainfall measured. It is observed a directly relationship between the rainfall and the capillarity tension and the volumetric water content.

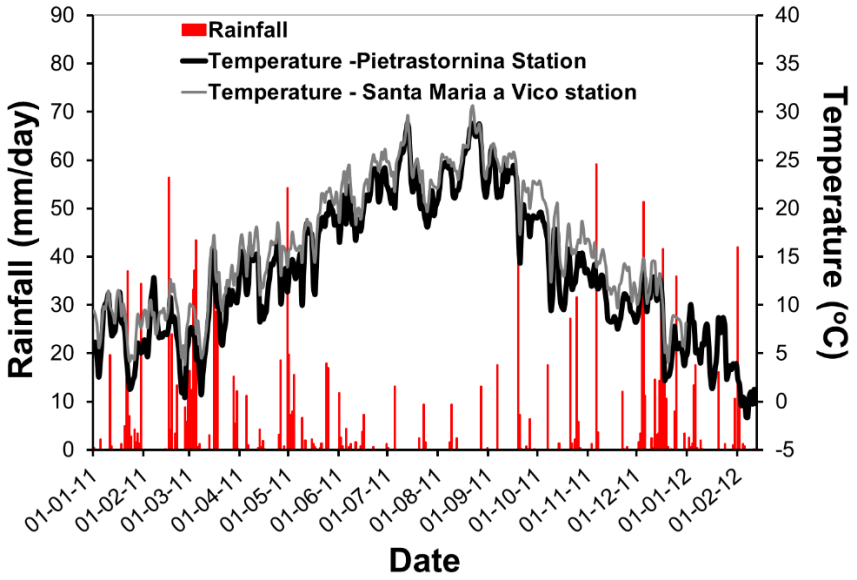

Figure 2-12 Climate data for Cervinara slope

On the other hand, it is detected that during the summer the hydraulic behaviour of the soil is controlled by the water level of the aquifer in the fractured limestone rock. In fFigure 2-13 is observed that for the summer months the suction value is higher for the deepest tensiometers. (Greco et al. 2013; Damiano et al. 2012; Comegna et al. 2013)

From June to August the data register by the TDR located at 1.00 m depth present a response that is inconsistent with the evolutions observed in the devices located above and below and the response observed with the tensiometers located at this depth. It is considered that the registration of this data present an error.

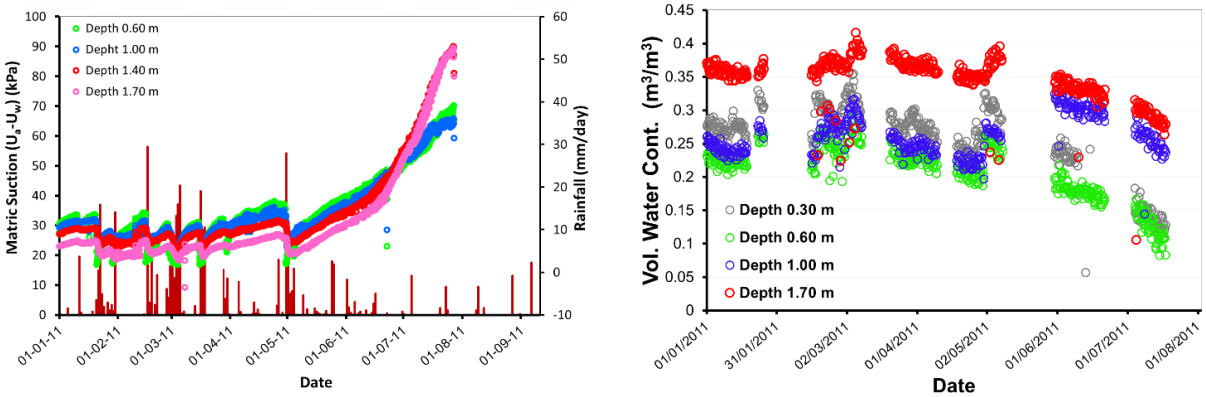

Figure 2-13 Slope response a) Matric suction b) volumetric water content

CHAPTER 3
CONCEPTUAL FRAMEWORK OF THE ANALYSIS.

The triggering processes presented in the landslides occurred in Cervinara region has been associated always to rainfall events. The rain-induce failure are mainly caused by the infiltration of the rainfall water. The evolution of liquid pressure within the slope depends on the characteristics of the rainfall, the material parameters such as: permeability, water retention curve, and consolidation parameters, and on the interaction with the atmosphere like infiltration, runoff, evaporation, and evapotranspiration. (Leroueil 2001)

The process that controlled the climatic actions include: the moist process, the radiation, heat exchange, the air mass motion and the interactions with the ground components like the vegetation. Figure 3-1 presents a scheme of the effects and interaction between the different fluxes, In general the atmospheric – soil interaction is controlled by the boundary condition fluxes (Noilhan & Planton 1989):

- The vapour flux: the sum of the evaporation (E) and the evapotranspiration (E_t).
- The energy flux: the addition of sensible heat (H_s), latent heat (H_c) and net radiation, R_n (function of the solar radiation (R_g), the atmospheric radiation (R_a) and surface radiation (S_r).
- The liquid flux: The addition of the precipitation (P), and runoff (R).

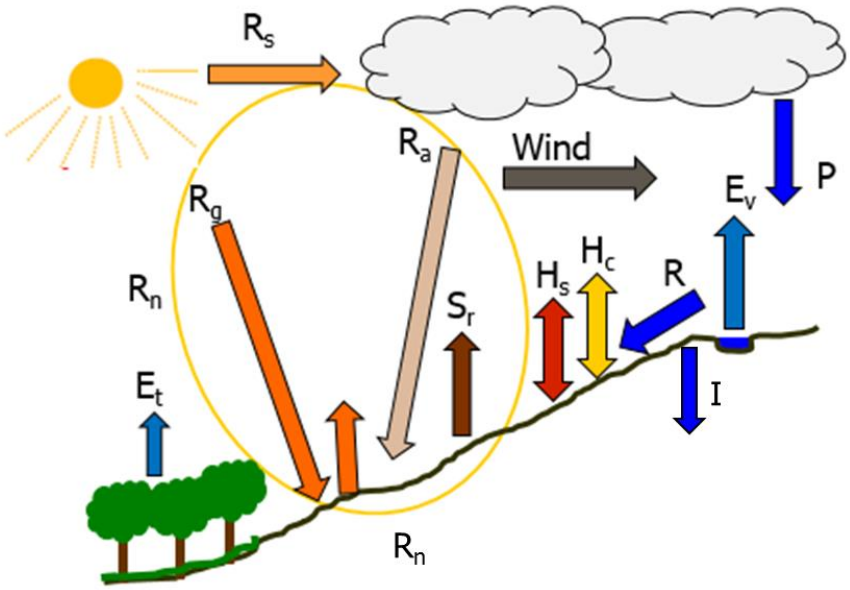

Figure 3-1 Fluxes involved in the soil-water-energy balance

The thermo-hydro-mechanical coupling process within the soil follows the physical laws that is presented next in a general point of view. The overall formulations are reported by Olivella et al. (1994) and Vaunat et al. (2012). Although, the problem to be analyse is related to the climatic actions and its mechanical effects, the coupling considered will be Hydro-Mechanical for the case of the flume test. Since the test is realise under isothermal conditions and Thermo-Mechanical for the real slope.

3.1 MATHEMATICAL FORMULATION OF THE COUPLED PROBLEM.

Partially saturated materials are three-phase media composed by solid, liquid and gas phases. The main species considered are: mineral (solid skeleton), water and air this last two can be presented even in liquid phase or gaseous phase like: the liquid water, dissolved air in water, water vapour or dry air.

The description of the Thermo-Hydro-Mechanical state of the partially saturated materials is defined by a set of state variables: Solid velocity ($\dot{u}_x, \dot{u}_y, \dot{u}_z$), liquid pressure ($p_l$), gas pressure ($p_g$) and temperature (T). Their evolutions are controlled by the balance equations (mass, heat, and momentum), the constitutive equations and the equilibrium restrictions. The complete formulation implemented in the finite element code CODE_BRIGHT is presented in Olivella et al. 1994

When a porous media is submitted to thermal, hydraulic and/or mechanical actions. They may have responses involving interactions between the different species that composed the media. For example, the thermal changes can generate the mechanical deformation due to thermal expansion of the solid and the water this generates an increasing in the saturation degree, due to the thermal expansion of the water. On the other hand, the process of flux of liquid phase is affected by the temperature due to the relation of the vapour diffusion and viscosity with temperature and to the mechanical changes due to the variation of porosity related to the mechanical deformations.

In addition to the main coupling the secondary coupling control the dependency of the materials and interstitial fluids parameters on the state variables. Figure 3-2 presents a scheme of the different coupling considered in the formulation of the THM model, distinguishing the main coupling and the secondary coupling (in italic in the figure). Is important to take in to account that all the coupling are not necessary to be active it depends on the characteristics of the problem. In unsaturated soils the deformation of the materials are related to the Terzaguhi´s effective stress $\sigma = \sigma - p_w$ giving the main coupling between the stress equilibrium and the water balance.

The balance equations allows interaction between the different phases and species. This equations are: the mass balance of each specie considered (solid skeleton, water and air), the balance of energy and the balance of momentum, which gives the stress equilibrium.

- Mass Balance:
  Water:

$$\frac{\partial}{\partial t}\left(\theta_l^w S_l \phi + \theta_g^w S_g \phi\right) + \nabla\left(j_l^w + j_g^w\right) + f^w = 0$$

Eq. 3-1

  Air:

$$\frac{\partial}{\partial t}\left(\theta_l^a S_l \phi + \theta_g^a S_g \phi\right) + \nabla\left(j_l^a + j_g^a\right) + f^a = 0$$

Eq. 3-2

  Solid:

$$\frac{\partial}{\partial t}(\rho_s(1-\phi)) + \nabla(j_s) + f^s = 0$$

Eq. 3-3

- Energy Balance:

$$\frac{\partial}{\partial t}\left(E_s\rho_s(1-\phi)+E_l\rho_l S_l\phi+E_g\rho_g S_g\phi\right)+\nabla\left(i_c+j_{Es}+j_{El}+j_{Eg}\right)+f^q=0$$

Eq. 3-4

- Balance of momentum

$$\nabla\sigma+b=0$$

Eq. 3-5

The notation employed in the balance equations is summarized in Table 3-1

Table 3-1 Notation for balance equations

Notation for balance equations	
θ_p^e	Apparent flux of the specie e in the phase p.
j_p^e	Flux of the specie e in the phase p.
S_l	Liquid saturated degree
S_g	Gas saturation degree
ϕ	Porosity
ρ_e	Density of specie e
E_e	Specific internal energy of specie e
i_c	Conductive heat flux
j_{Ep}	Energy flux in phase p
f	Source/ sink term
σ	Stress tensor
b	Body forces
	Species (e): Water (w), Air (a), Soil (s)
	Phases(p): Water (w), Air (a), Soil (s)

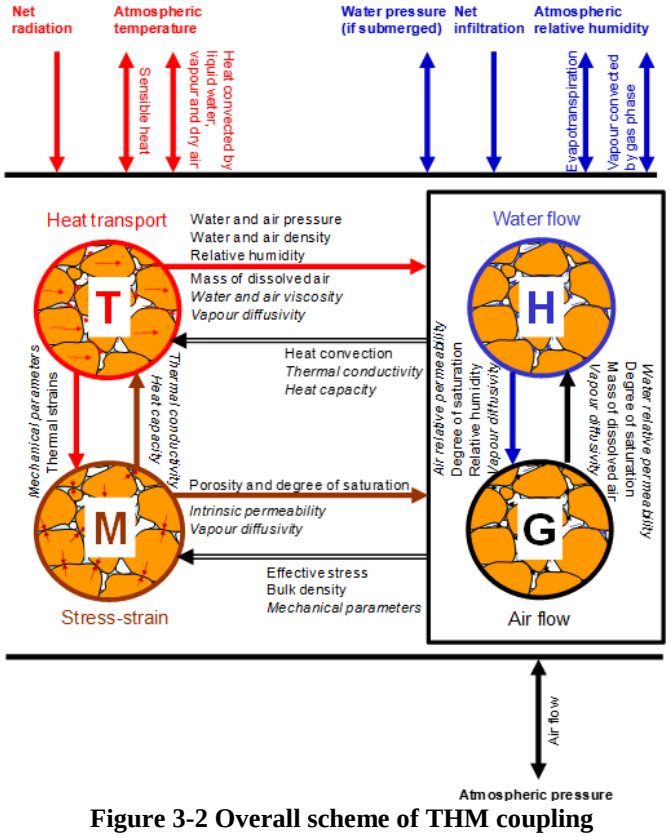

Figure 3-2 Overall scheme of THM coupling

As presented by Olivella et al. (1996) the balanced equations formulated are define in terms of unknown variables which are related with the state variables through the constitutive equations and equilibrium restrictions. Which in many cases constitute the secondary coupling. Table 3-2 present a list of principal constitutive equations and equilibrium restrictions.

Moreover, to complement the problem is important to consider the boundary conditions and restrictions which are added to the mathematical problem as nodal fluxes or tensions. The proposed THM formulation allows to apply several conditions at the boundaries of the problem: displacement, temperature, liquid and gas pressures or, forces and fluxes.

Table 3-2 Constitutive equations and equilibrium restrictions

Equation	Variable name	Variable
Constitutive equations		
Darcy´s law	Liquid and gas volumetric flux	$q_l\, q_g$
Fick´s law	Diffusive flux of vapour	i_g^w
Fourier´s law	Conductive heat flux	i_c
Retention curve	Liquid phase degree of saturation	S_l
Mechanical constitutive model	Stress tensor	σ
Phase density	Liquid density	ρ_l
Gas law	Gas density	ρ_g
Equilibrium restrictions		
Henry´s law	Air dissolved mass fraction	w_l^a
Psychrometric law	Vapour mass fraction	w_g^w

The formulation presented before is supplemented with the mechanical constitutive model CASM developed by González (2011) an enhanced formulation of the original CASM model established by Yu (1998). This mechanical model includes the dependency of the yield envelope of the material on suction according to the framework developed by Alonso et al. (1990). An interesting feature of this model is the flexible definition of the shape of the yield envelope presented by Eq. 3-6 that allows a well-reproducing the shear strength of the material on the dry side of the critical state.

$$f = \left(\frac{\sqrt{3}\,J}{M_\theta(\bar{P}+P_s)}\right)^n + \frac{1}{\ln r}\ln\left(\frac{\bar{P}+P_s}{P_c+P_s}\right)$$

Eq. 3-6

Where, $\bar{p}$ is the mean net stress, J is the square root of the second stress invariant of deviatoric stress tensor, Mθ the slope of the critical state line as a function of Lode angle, P_c is the presconsolidation value , P_s is a tensile strength due to s suction, the variation of P_c and P_s with suction, follows the formulation described in Alonso et al. 1990. Finally, the parameters n and r refer to the shape and size of the yield surface. The parameter n specify the shape of the yield surface while r is a spacing ratio which controls the location of the intersection of the critical state line with the yield surface.

3.2 DOUBLE-POROSITY WATER RETENTION CURVE.

The volcanic ashes of the Cervinara slope present an important percentage of sandy component with a significant amount of non-plastic silt. This material is characterized by the presence of intergranular and intragranular pores. During SEM observations was found that the itergranular pores have a size comparable to that found in coarsest particles. (Olivares & Tommasi 2008). For this reason is concluded that this soil is characterized by a bimodal pore size distribution.

According to Casini et al. (2012) the heterogeneity of the pore size distribution has an effect in the water retention properties. Although the water retention curve for different type of soils is well fitted with a Van Genuchten curve, for this kind of materials is more realistic if is used a multimodal retention model. Defined as a linear superposition of sub-curves of the Van Genuchten type defined by Eq. 3-7

$$\frac{e_w + e_{wres}}{e - e_{wres}} = \sum_{i=1}^{k} w_i \left[\frac{1}{1 + (\alpha_i s)^{n_i}}\right]^{m_i}$$

Eq. 3-7

Where e_w is the water ratio (Sr e), k the number of sub-curves, w_i the weighting factors for each sub-curve, and $\alpha_i, m_{i,}, n_i$ are the parameters for each sub-curve.

The Water retention curve plays an important role in the formulation used. It enable to calculate the value of liquid saturation degree employed in the water and air mass balance and in the energy balance. For this reason is very important to obtain the most realistic water retention curve.

Therefore, the water retention curve implemented in the formulation follows the idea of the multimodal retention curve for two pore sub-systems or curves. Identified are micropores or intragranular and macropores or intergranular. The bimodal water retention curve follows the Eq. 3-8

$$S_e = \frac{S_l - S_{rl}}{S_{ls} - S_{rl}} = (1 - w)\left[1 + \left(\frac{P_g - P_l}{P}\right)^{\frac{1}{1-\lambda_M}}\right]^{-\lambda_M} + w\left[1 + \left(\frac{P_g - P_l}{P_m}\right)^{\frac{1}{1-\lambda_m}}\right]^{-\lambda_m}$$

Eq. 3-8

$$P = P_{0M}\frac{\sigma}{\sigma_m}\ , P_m = P_{0m}\frac{\sigma}{\sigma_m}$$

Where w is the weight factor for the micro, P_{0m}, P_{0M} are the values for the air entry values for the micro and macro respectively,λ_m, λ_M the parameters related to the shape of the retention curve for the micro and macro respectively. S_l the saturation degree, S_{ls} the maximum saturation degree and S_{rl} the residual saturation degree. Figure 3-3 present the bimodal water retention curve obtain for the laboratory data presented in section 2.1.1. This water retention curve is compared with a Van Genuchten approximation (monomodal water retention curve) as was expected the more realistic approximation is achieved with the bimodal water retention curve.

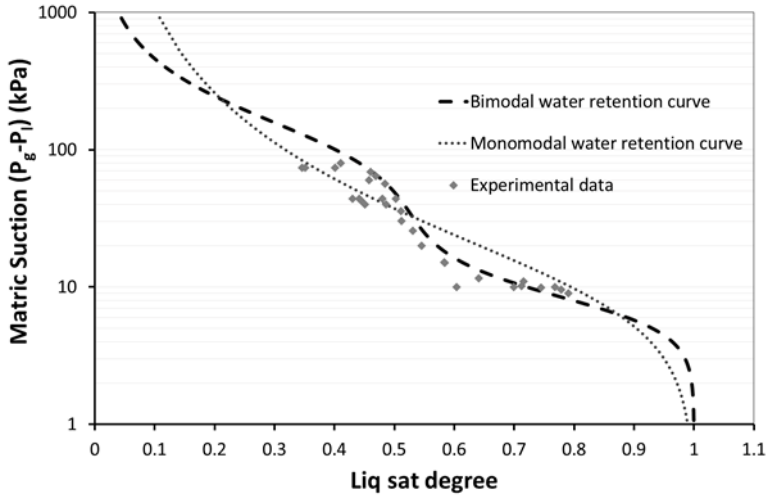

Figure 3-3 Bimodal water retention curve

3.3 ATMOSPHERIC BOUNDARY CONDITION.

The atmospheric and vegetation actions encompass mass and heat exchanges at the ground surface. Including evaporation, rainfall, radiation and sensible heat (see Figure 3-1). Additionally the vegetation boundary condition consider transpiration and heat exchanges.

According to Vaunat et al. (2012), the energy received by the soils come from the sun radiation which is a shortwave radiation. At the top of the atmosphere the incident solar radiation (R_s) depends on: the energy emitted by the sun (1376 W/m^2), the distance between the sun and the earth, the latitude and the current time. The atmosphere and clouds reflect and absorbed part of the incident radiation. For that reason the radiation at soil surface (R_g) is lower than R_s. The relation between R_g and R_s depends on: the cloudiness, the atmosphere absorptivity, and the travel length across the atmosphere that depends on the latitude and current time.

Additionally, the radiation absorbed by the clouds is released with direction to the space and with direction to the earth (R_a) but in the shape of long wave radiation. The ground surface receives both type of radiation waves. Finally part of the energy is reflected by the soil based with the albedo of the surface. Defined as the radio between the incident wave and the reflected wave which depends on characteristics of the surface such as colour or material. The albedo is also influenced by the saturation degree of the material since the albedo of the water is two times lower that the albedo for the dry soil.

The remaining part of the energy is stored in the soil some of this energy is released to the atmosphere by convection and the soil radiation. Moreover, the difference between the ground surface and the atmosphere produces the conductive flux, the advection flux and the heat transport through the mass fluxes that cross the surface like: air, liquid water or vapour. Finally the soil radiation (S_r) that is a long wave radiation is control by the emissivity of the soil. On the other hand the energy that is not released to the atmosphere controls the temperature changes of the soil which has an important role in the evaporation of water.

In bare grounds, the evaporation is given by the difference of water potential between the atmosphere (vapour) and the soil (liquid and vapour). While this two potential not be in equilibrium there is vapour diffusion from the soil to the atmosphere this effects are also controlled by the aerodynamic effect of the wind. Besides that, within the soil the potential of liquid and gas phase of the water must be in equilibrium generating the evaporation of liquid

water. However, the change of phase process consumes heat so the process will be also conditioned to the energy availability.

Penman, (1948) introduce the concept of potential evaporation. In order to obtain a rational approach for the maximum value of evaporation based on the availability of heat in the medium. This concept is true for irrigated fields or wet climates but for semi-arid and non-irrigated areas the evaporation will be imitated by the availability of water. In this cases the actual evaporation will be lower than the potential evaporation.

Another important contribution for hydric balance in the vadose zone is the net infiltration which is the amount of rain water that do not is intercepted by the vegetation, evaporated or come into runoff. The infiltration rate depends on: the inclination of the slope, the state of compaction of the surface, and the moisture content of the material (Blight 1997)

The vegetation plays an important role in the hydric balance. Very important in zones with an important presence of vegetation like the case of Cervinara region. The transpiration process of the plants which basically consist in the vaporization of the liquid water at the plant leaves to the atmosphere. This water is previously absorbed from the soil by the roots plants. Is important to take into account the difference between the evaporation and transpiration, the first one is the process whereby the liquid water convert in to vapour at the ground surface. The water can be evaporated from different surface such as lakes, rivers, pavements or soils. While the transpiration is just the liberation of vapour from the plant.

Therefore, when the herbage is small the water lost correspond basically to the evaporation process but once it grows the transpiration will be predominant. Basically the vegetation acts as bypass between the soil surface and the deepest zone of direct evaporation. The main factors that influence the transpiration rate are: water and energy available in the soil, leaf and root density, root depth, vegetation type, atmosphere relative humidity and temperature.

The most important changes in water content normally occur close to the surface. In the first meters called active zone the water potential varies between negative values (suction) during dry periods to lightly positive values during wet seasons. The fluctuations of water pressure underneath of the active zone act as the response to the solicitations generated in the active zone in absence of other effects or solicitations.

The variations in pore water pressure. For instance, in suction values are highly influenced by changes in the flux boundary conditions. They are: infiltration, evaporation and transpiration which are controlled by the climatic actions. According to Leroueil (2001) the infiltration in unsaturated soils is more complex than in saturated soils, because the initial conditions depend in antecedent hydrological conditions and the parameters that control the infiltration in soils such as water retention curve and hydraulic conductivity depend on soil suction.

The atmospheric process and vegetation present a very complex behaviour. For this reason with the aim of a geotechnical modelling some simplifications has to be considered. Mainly the model do not consider the atmosphere as a hole but as combination of fluxes acting at the soil surface as a boundary condition. On the other hand, vegetation is considered as a nonlinear sink term of water mass applied at a defined depth (root depth). Additionally, the atmospheric boundary condition has to be compatible with the formulation that controls the behaviour in the soil which should be able to consider the Thermo-hydro-mechanical coupling presented before. The formulation for the atmospheric boundary condition considered in the atmospheric –

vegetation module of CODE_BRIGHT is summarized hereinafter. Figure 3-4 presents a scheme of the different fluxes considered in the atmospheric boundary condition

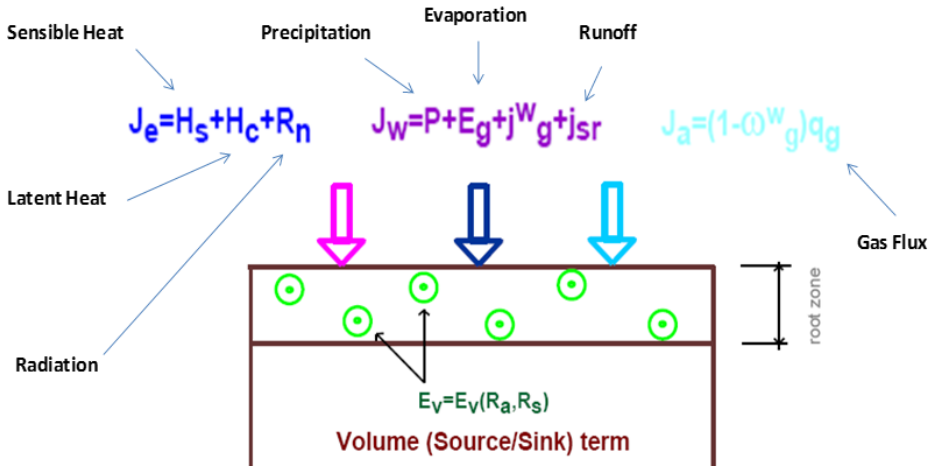

Figure 3-4 Scheme of flux involved in the atmospheric boundary condition

3.3.1 Gas flux.

The gas flux is controlled by the Darcy´s law, in terms of the atmospheric pressure (Pat) is:

$$q_g = \gamma_g \left(P_g - P_{at}\right)$$

Eq. 3-9

Where γ_g is the leakage coefficient, and P_g is the gas pressure. This flux carries two species dry air and vapour, the dry air flux is represented by Eq. 3-10 where w_g^w is the mass fraction of vapour.

$$J_a = (1 - w_g^w) q_g$$

Eq. 3-10

3.3.2 Flux of water.

The flux of water at the surface is given by the sum of: precipitation P, ground evaporation E_v, the advective flux of vapour J_g^w and the surface runoff J_{sr}. Is important to take in to account that the precipitation considered is the difference between the real precipitation and the part intercepted by the rainfall.

$$j_w = P + J_g^w + E_v + J_{sr}$$

Eq. 3-11

The evaporation is presented by Eq. 3-12. Where veg is the vegetation fraction defined as the greened area per unit of area of ground, r_a is the aerodynamic resistance, ϕ is the stability factor, κ is the von Karman´s constant (generally 0.4), v_a is the wind velocity, z_0 is the ground surface roughness associated to the canopy height, z_a is the screen height at which the values of wind

velocity and atmosphere absolute humidity (ρ_{va}) are measured, and ρ_v is the absolute humidity of the soil.

$$E_v = (1 - veg)\frac{1}{r_a}(\rho_{va} - \rho_v) \qquad r_a = \frac{\left(\ln\left(\frac{z_a}{z_0}\right)\right)^2}{k^2 v_a \phi}$$

Eq. 3-12

The advective flux of water, is evaluated by

$$j_g^w = \begin{cases} w_g^w \, q_g & if \; P_g > P_{ga} \\ \rho_{va}/\rho_{ga} \; q_g & if \; P_g \leq P_{ga} \end{cases}$$

Eq. 3-13

Finally the surface runoff is defined as the flow rate of water that do not is infiltrated into the soil. For this reason is considered that infiltration only occurs when the atmospheric pressure (P_{ga}) is higher than the ground pore pressure (P_l) in which case the surface runoff will be null, see Eq. 3-14 where γ_w is the ground surface liquid leakage coefficient.

$$j_{sr} = \begin{cases} \gamma_w \, (P_l - P_{ga}) & if \; P_l > P_{ga} \\ 0 & if \; P_l \leq P_{ga} \end{cases}$$

Eq. 3-14

3.3.3 Flux of energy.

The flux of energy is determined by the sum of: the sensible heat (H_s), the heat flux convected by the mass fluxes (Hc) (the most important is the latent heat of vaporization carried by water mass flux) and the net radiation (R_n). See Eq. 3-15

$$J_e = H_s + H_c + R_n$$

Eq. 3-15

The sensible heat is calculated through the aerodynamic diffusion relation. Presented in Eq. 3-16 where C_a is the specific heat of gas, ρ_{ga} is the atmospheric gas density, T_a the atmospheric temperature, $T_0$the soil temperature, and r_a is the aerodynamic resistance previously described.

$$H_s = \rho_{ga} C_a \frac{1}{r_a}(T_a - T_0)$$

Eq. 3-16

On the other hand, the convected heat flux is computed taking into account the internal energy of liquid water, vapour and air, according to:

$$H_c = h_v\left(E_v + J_g^w\right) + h_{la}(P + J_l^w) + h_{a0} J_a$$

Eq. 3-17

Where, J_l^w is the flux of water in liquid phase, P is the precipitation, J_a is the flux of air and h_v, h_{la} and h_{a0} are the free energy of vapour, liquid water and air. Finally the net radiation is the part of heat flux that considers the solar and atmospheric radiation given by Eq. 3-18

$$R_n = (1 - A_l)R_g + \varepsilon\, R_a - S_r$$
$$S_r = \varepsilon \sigma_s {T_a}^4$$

Eq. 3-18

For the calculation of R_n. R_g is the solar short wavelength radiation, R_a is the long wavelength atmospheric radiation, σ_s is the Stefan-Boltzman constant (5.67×10^{-8} J s^{-1} m^{-2} K^{-4}), ε is the ground emissivity and A_l is the albedo of the soil, this last two parameters are function of the degree of saturation (S_l), according to:

$$A_l = A_d + (A_d - A_w)(S_l^2 - 2S_l)$$
$$\varepsilon = 0.9 + 0.05 S_l$$

Eq. 3-19

Where A_d and A_l are the dry and wet albedo. The atmospheric log wavelength radiation could be measured in the field. In case that this data are not available the atmospheric radiation R_a can be estimated as a function of the atmospheric temperature and the atmospheric absolute humidity according to Eq. 3-20

$$R_a = \sigma_s\, {T_a}^4 \left(0.605 + 0.048\sqrt{1370\rho_{va}} \right)$$

Eq. 3-20

In order to calculate the values for direct solar radiation R_g a sinusoidal function presented in Eq. 3-21 could be used. d_s is the time span between the sunrise and sunset, t_m is the time at noon and R_G is the daily solar radiation calculated thought an empirical relation as function of the latitude, the index cloud and current date.

$$R_g = \begin{cases} \dfrac{\pi\, R_G}{2\, d_s} \sin\left(\dfrac{(t - t_m + 0.5 d_s)\pi}{d_s} \right) & \text{if } t_m - 0.5 d_s \le t \le t_m + 0.5 d_s \\ 0 & \text{otherwise} \end{cases}$$

Eq. 3-21

3.3.4 Evapotranspiration.

The transpiration is the process whereby the plant loss vapour of water from the leaves or another aerial part of the plant. This water is previously took from the soil by the roots. This process occurs due to the gradient in relative humidity between the plant and the atmosphere. The plant control this flux through chemo-thermo-hydraulical actions at cell level. For that reason the modelling of this process is very complex.

The general approach widely used in agricultural engineering considers the modelling of transpiration by applying the effect of this release vapour at canopy level (Sellers et al. 1986). According to Noilhan & Planton (1989) this effect depends on the difference between the vapour density of the atmosphere (ρ_{va}), and the leaf. Since the relative humidity within the leaf is close to 100%, the vapour density at the leaf is considered as saturated (ρ_{vasat}) which depends only in the temperature. The transpiration is computed as:

$$E_t = veg\, \frac{1}{(r_a - r_s)}\, (\rho_{vasat} - \rho_{va})$$

Eq. 3-22

Where r_a is the aerodynamic resistance and veg is the vegetation fraction both parameters previously described, r_s is the leaf resistance defined as the resistance to the transfer of water from the root zone to the leaf surfaces. Calculated according to Eq. 3-23

$$r_s = \frac{r_{smin}}{LAI}\left[\frac{F_1}{F_2\ F_3\ F_4}\right]$$

Eq. 3-23

Where r_{smin} is the minimum surface resistance, which is depends on the type of plant. It is considered a maximum value of surface resistance (r_{smax}) of 5000 s/m. LAI is the leaf area index, defined as the area cover by leaves per square meter of ground. In general terms the relation $r_{smin}/_{LAI}$ remains constant. Finally, F_1, F_2, F_3 and F_4 are functions widely used in agricultural engineering defined as presented below

$$F_1 = \frac{1 + \left(\frac{2}{LAI}\ \frac{0.55\ R_g}{R_{gl}}\right)}{\left(\frac{1.1}{LAI}\ \frac{R_g}{R_{gl}}\right) + \frac{r_{smin}}{r_{smax}}}$$

Eq. 3-24

The function F_1 considers the influence of the photosynthetically active radiation equal to 0.55 R_g. R_{gl} represents the maximum value for R_g 30 W/m^2 for the cases of the forests this is the case of the Cervinara region. The function F_2 represents the capacity to extract water from the soil depending on the water content (θ), according to Eq. 3-25

$$F_2 = \begin{cases} 0 & if\ \theta \le \theta_w \\ \dfrac{\theta - \theta_w}{\theta_{fc} - \theta_w} & if\ \theta_w \le \theta < \theta_{fc} \\ \dfrac{1 - \theta}{1 - \theta_a} & if\ \theta \ge \theta_a \end{cases}$$

Eq. 3-25

Where, θ_w is the water content at the wilting point it is the threshold below plants cannot extract more water from the soil. Noilhan & Mahfouf (1996) consider that this value corresponds to a suction value of 1.5 MPa. θ_{fc} represents the field capacity which is the water content remaining after a downward gravity drainage correspond to a low value of hydraulic conductivity (0.1mm/day) (Noilhan & Mahfouf 1996). This parameter is also associated to a value of suction between 0.01 to 0.05 MPa. Finally θ_a is the anaerobiosis point that represent the water content at which the metabolism of the plant begging to loose efficiency.

Function F_3, considers the effect of atmosphere vapour pressure deficit which is very important because when this happens the stomata close. In eEq. 3-26 γ is an empirical parameter.

Last but not least, function F_4 introduces the dependence in air temperature governed by Eq. 3-27.

$$F_3 = 1 - \gamma\ (\rho_{vasat} - \rho_{va})$$

Eq. 3-26

$$F_4 = 1.0 - 0.0016(298 - T_a)^2$$

Eq. 3-27

CHAPTER 4
NUMERICAL MODELS

The slope failure in unsaturated soils is controlled by the characteristics of: water flow, pore-water pressure, and shear strength of the soils. These parameters are highly influenced by the flux boundary conditions like: precipitation or evaporation. In general the rainfall-induced landslides are basically determined by the infiltration of water in the materials however this process is very complex

The objective of the Round Robin test is to carry on a benchmark exercise in which modellers be able to considering information at different scales of observation. As well as the capability of reproducing the response and make predictions taking into account the complexity of the process developed during the rainfall-induced landslides.

The numerical models were developed with the finite element method formulation, CODE-BRIGHT settled by the department of geotechnical engineering and geo-sciences (UPC) (Olivella et al. 1994) to model Thermo-Hydro-Mechanical problems in geological media. The atmosphere and vegetation contributions were modelled by a special flux boundary condition recently implemented (Saaltink et al. 2011). The formulation considered was presented in chapter 3.

In order to maintain the intention of the benchmark exercise the numerical simulations were developed considering the same scales of observations considered: laboratory experiments, flume infiltration test and field slope, as is presented hereinafter.

4.1 LABORATORY SCALE.

The laboratory experiments are realized in order to establish at small scale the parameters that will control the soil behaviour. Section 2.1.1 presents the basic results of the test performed to the Cervinara ashes. One of the tests performed is the suction controlled triaxial test which gives an idea about the resistance of the soil. The adequately understanding and modelling of this test will provided the shear strength parameters that control the failure of the soil under unsaturated conditions.

For the modelling of the suction controlled triaxial test three stages were considered. First the sample is submitted to an isotropic stress, then the suction is imposed and finally the sample is load at constant strain rate. In total 6 different test were evaluated which characteristic are listed in Table 4-1

Table 4-1 Suction controlled triaxial test characteristics

Test	Sample depth (m)	Initial Suction (kPa)	Suction imposed (kPa)	Isotropic stress (kPa)
1Cu1040	3.5	10.0	11.0	28.8
C4P1USP	4.0	9.0	44.0	60.0
C22USP	3.5	10.5	43.0	90.1
C70USP0	3.5	11.05	74.0	89.3
C62USP	1.0	14.0	74.0	22.43
C61USP1	1.0	15.0	44.0	23.0

The modelling of these tests is developed employing a hydro-mechanical coupling over a 2D model considering a vertical symmetric axis. Figure 4-1 Model boundary conditionspresents a

summary of all boundary conditions considered during the calculation of the suction controlled triaxial test. The mechanical model considered is the CASM model (González 2011) and the water retention curve correspond to a bimodal water retention curve presented in Figure 3-3. Additionally the intrinsic permeability correspond to the mean value obtained during the experimental test (1.44 e-13 m^2). Table 4-2 presents the parameters considered

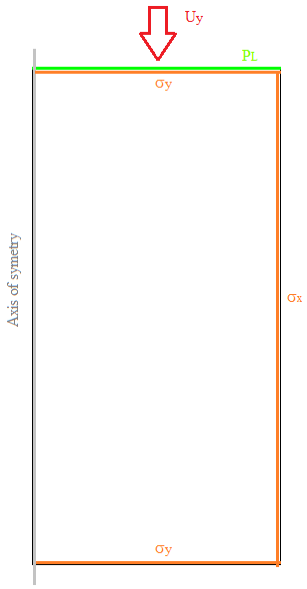

Figure 4-1 Model boundary conditions

Table 4-2 Mechanical and Hydraulic parameters.

Mechanical data				**Hydraulic data**			
General parameters		Specific parameters		Retention curve		Intrinsic permeability	
ν	0.3	P_r (MPa)	0.005	P_{0M} (MPa)	0.0075	Darcy´s law	
κ	0.035	r_{lc}	0.95	λ_M	0.7	K (m^2)	1.44e-13
λ	0.25	β	50	P_{0m} (MPa)	0.120	Liq. phase rel. Permeability	
r	2	κ_s	0.04	λ_m	0.55	Generalized power function	
n	2	k_s	0.13	w	0.53	A	1
M	1.32			S_{rl}	0	λ_{rp}	4.5
ϕ_{cs}	32.8			S_{ls}	1		

The principal result obtained from this test is the evolution of the deviatoric stress with the axial deformation presented in Figure 4-2. Is important to observe that the behaviour of all the cases is satisfactorily reproduced by the model even for the case of the test 1Cu1040 which present a peak response. In all the cases the value of final stress is well obtain, even so, in some test the value is reached earlier than in the test. This is due to the value of λ considered correspond to the value obtained with the compressibility test presented in section 2.1.1. In general the values of λ obtained with the compressibility test are lower that the values observed during test like the triaxial test.

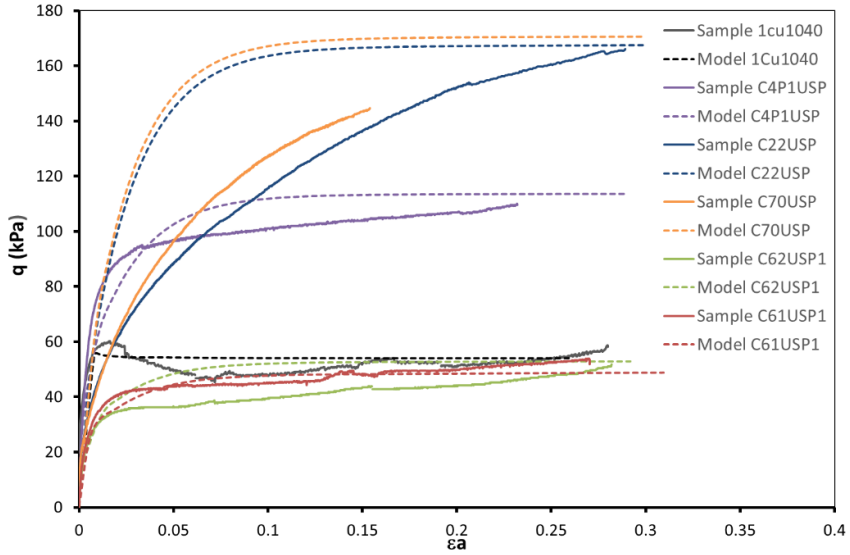

Figure 4-2 deviatoric stress vs εa.

Aditionally, to evaluate the hydraulic response of the material. Is important to observe the evolution of water content during the equilibration of suction phase. For this stage the unique process involved is the hydraulic. Figure 4-3 presents the results achieved where dw represent the variation in water content. It is concluded that with the hydraulic parameters considered the evolution of water content is adequately reproduce by the modelling.

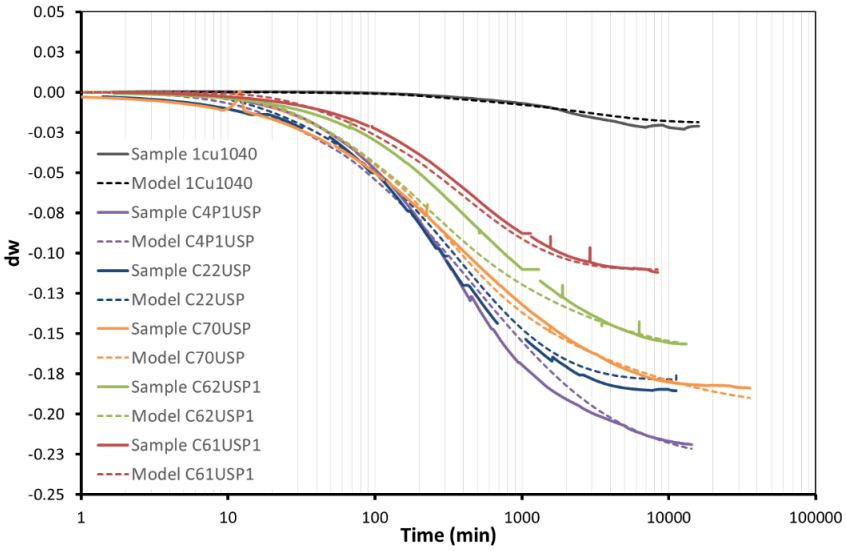

Figure 4-3 water content variation

Is interesting to evaluate the effect of the stress path imposed to the samples in the evolution of the yield surface described by González (2011) and Alonso et al. (1990). To complemente the mechanical parameters presented in Table 4-2 is necessary to determinate the value for the preconsolidation stress at saturated conditions (P_0). This material is considered as normally consolidated. Which means that the precosolidation stress (P_c) depends only in the current stress condition at the samples extraction depths. For samples extracted at 1m the pre-consolidation stressnat saturated conditions considered is 28 kPa and for samples taken between 3.5m and 4m the value considered is 60 kPa.

As was presented before the stress path considered correspond to 3 different stages/paths:

1. The sample is load under an isotropic stress.
2. The suction desired is imposed, maintaining the stress.
3. The sample is load at constant strain rate (2.33e-6 m/s) maintaining the stress.

For unsaturated materials the yield surface is defined in a three-dimensional space composed by: the mean stress (P), the deviatoric stress (Q) and the suction (S). The variation of this surface is presented in two different planes: the P vs Q and the plane P vs S.

Two different cases are considered as example to see the evolution of yield surface. The sample C70USP presented in Figure 4-4 and sample C61USP presented in Figure 4-5. This two samples were extracted at two different depths the first one at 3.5m depth while the second one at 1m. For this reason the preconsolidation stress considered are different.

Taking into account, the values of preconsolidation stress and the characteristics of the tests presented in Table 4-1 (row 4 and 6). It is observed that for sample C70USP the path 1 (load under isotropic stress) generates a change in the LC curve. While for sample C61USP this process is developed in the elastic zone consequently without generating any change in the yield surface. For that reason the LC after the path 2 is equal to the initial LC. Hence the increment in suction maintaining the value of mean stress do not affect the yield surface it occurs under elastic conditions.

Finally for the load at constant strain rate (stage 3) is observed that for sample C70USP this process is developed under the plastic zone as is shown in Figure 4-4a. While for sample C61USP the begging of this load process is settled in the elastic zone presented in Figure 4-5a. The difference of the response is appreciated in the figure of the deviatoric stress vs axial strain, (Figure 4-4c and Figure 4-5c) where is apreciated that for the sample C61USP the initial strains present a linear relation with the deviatoric stress. That is to say elastic strains which are control by the parameter of load/reload (κ). Although, for sample C70USP this relation is not linear since the begging of the load stage, this means that the strains are plastic from the beginning of the phase.

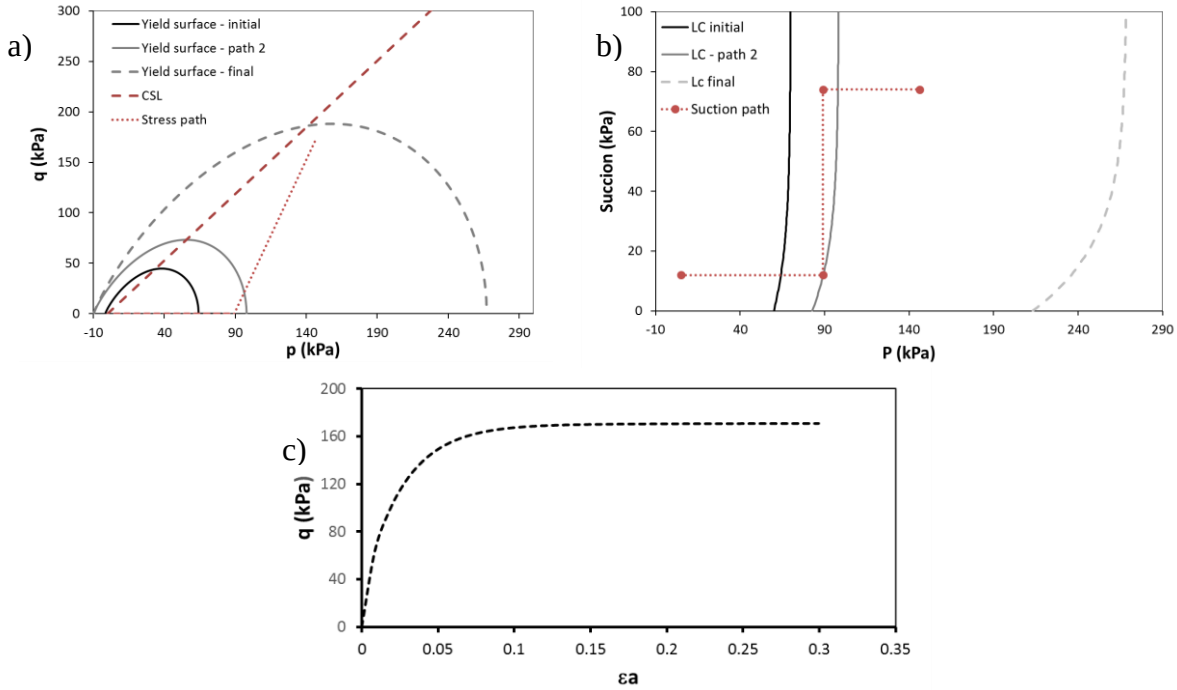

Figure 4-4 Yield surface variation for sample C70USP. a) p vs q plane b) p vs suction plane a) q vs axial strain

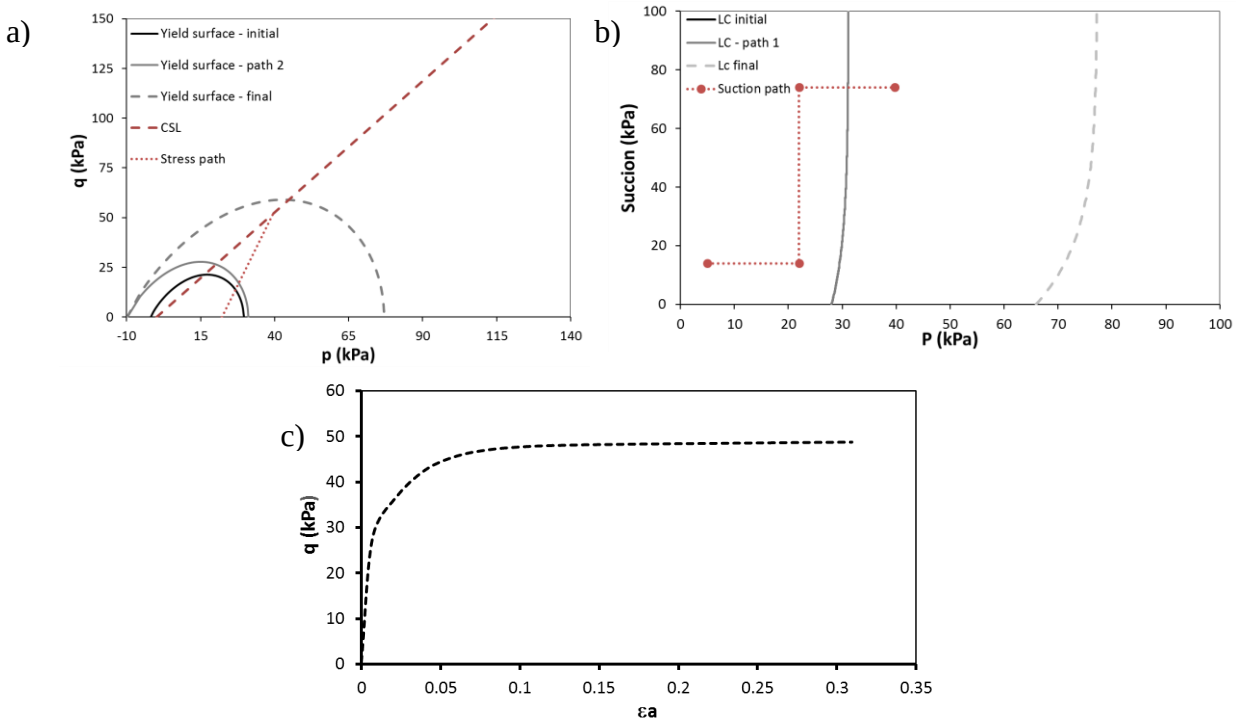

Figure 4-5 Yield surface variation of sample C61USP a) p vs q plane b) p vs suction plane a) q vs axial strain

In order to model the test the most realistic possible during the final stage (the load under constant rate strains) the constant value of suction was imposed as a boundary condition at the top of the sample. For that reason, is very interesting to evaluate the variation of suction during this stage shown in Figure 4-6. When the sample is load the deformation generated produced a reduction in the air volume in the sample. Therefore, the porosity decrease leading to a fall in the values of suction but as the value of suction is been imposed at a boundary of the sample.

The variation of suction reaches a constant value as an equilibration of both process: the mechanical and the hydraulic.

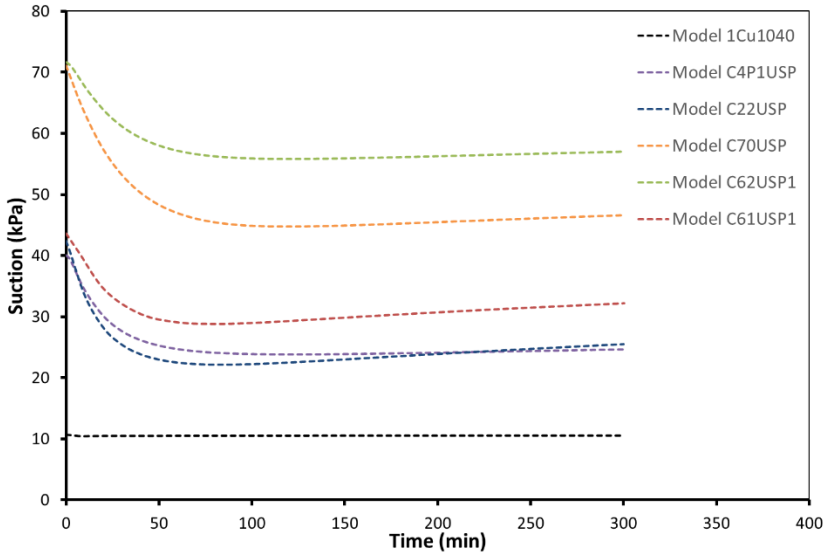

Figure 4-6 variation of suction during load under constant strain rate

4.2 FLUME TEST.

The flume test consist in a mock up experiment over a slope model design to investigate the mechanism of failure of the rainfall-induced landslides. For this reason the flume is highly equipped with instrumentation devices. In fact during the test the values of: suction, water content profiles, liquid pressure and settlements are measured. The complete description of the instrumentation and the test procedure is presented in section 2.1.2.

As is presented in section 2.1.2 the method used to create the slope is the moist tamping. This process consist in the creation of the sample by layers. The material of each layer is deposited and then is compacted by applying a quasi-static load until the material reach the volume needed according to the value of porosity desired. (Frost & Park 2003).

Additionally, at least one of the minitesiometers installed is located in the profile where the values of water content are measured allowing to relate this two values. Which present an idea of the water retention curve for this tests. Figure 4-7 presents the water retention curve obtain for the flume test based with the data obtained from the minitensiometers T3 in test D3 and minitensiometers T4 and T6 in test D4.

The water retention curve obtained from the laboratory tests present a value of air entry higher than the value obtain from the flume test response. This variances are attribute to the differences in density and anisotropy. Besides that is very difficult to recreate the large pores in the recreation of samples like is the case of the moist tamping procedure. Similar responses are presented in Askarinejad et al. (2011) and Askarinejad et al. (2012).

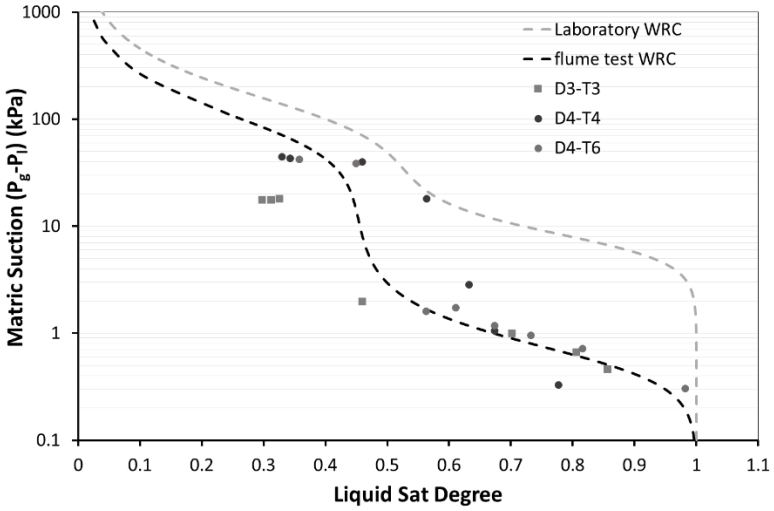

Figure 4-7 Flume test water retention curve

Beyond the difference with the data obtain in the laboratory tests. It is important to take into account that the results obtain from test D3 and test D4 present a discrepancy especially for higher values of suction. For a saturation degree of 0.3 test D3 present lower values of suction than for test D4 this difference could lead to differences in the value of the initial saturation degree during the modelling.

According to Askarinejad et al. (2012) the hydraulic conductivity of unsaturated soils is function of the pores structure and the relative amount of pore fluid in the system. For this reason this parameters can vary from: reconstituted samples, undisturbed samples and in situ conditions. The value of intrinsic permeability was calibrated trough back analysis. Moreover taking into account the Kozeny´s equation the relation between the intrinsic permeability and the porosity for the flume test analysis is obtained and is presented in Figure 4-8.

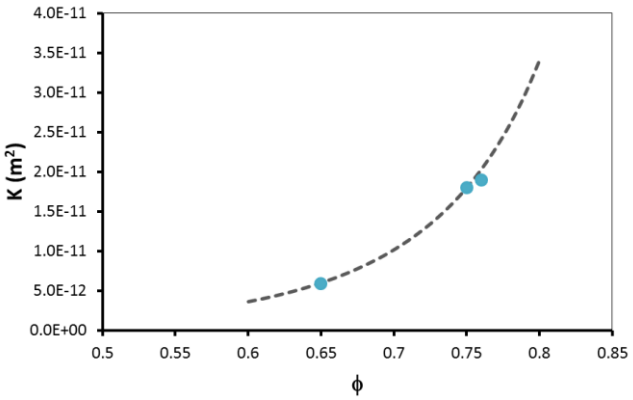

Figure 4-8 Intrinsic permeability considered for flume test analysis.

The mechanical parameters considered correspond to the parameters obtained from the laboratory experiments more specifically from the suction controlled triaxial tests presented in section 4.1, Table 4-3 presents a summary of the parameters considered.

Table 4-3 Mechanical and hydraulic parameters - flume test

Mechanical data				Hydraulic data			
General parameters		Specific parameters		Retention curve		Intrinsic permeability	
ν	0.3	P_r (MPa)	0.0005	P_{0M} (MPa)	0.0006	Darcy´s law	
κ	0.035	r_{lc}	0.95	λ_M	0.6	K (m^2) ϕ=0.75	1.8e-11
λ	0.25	β	50	P_{0m} (MPa)	0.080	K (m^2) ϕ=0.76	2.0e-11
r	2	κ_s	0.04	λ_m	0.55	K(m^2) ϕ=0.65	5.9e-12
n	2	k_s	0.13	w	0.45	Liq. phase rel. permeability	
M	1.32			S_{rl}	0	Generalized power function	
ϕ_{cs}	32.8			S_{ls}	1	A	1
						λ	4.5

The values considered for the initial stress and pre-consolidation stress are crucial to reproduce adequately the mechanical response of this test. Especially because the failure is not caused by the imposition of a stress but, due changes in suction. The value of initial stress and pre-consolidation stress will determine the proximity to yield stress and for instance the failure time.

To achieve this values the process of production of the slope was modelled. For this purpose a horizontal flume have been considered with the same measures of the final flume but with an initial porosity higher than the value reported as initial for the soaking test. This value has been supposed because it was not measured. Then this flume is subjected to a static load later the load is removed. The value of load imposed was calibrated with the final value of porosity which should be equal to the porosity of the test. Is very interesting to observe that this process generate an anisotropic distribution of tensions generating a higher value of stress in the horizontal direction.

Although, the phenomena analyses correspond to a mechanical failure due to the soaking process (hydro-mechanic process) 2 different types of 2D models were considered to evaluate the performance. The first one considers just the hydraulic process and the second one contemplates the hydro-mechanical coupling. This two models are developed especially to see the effect of the mechanical coupling over the hydraulic process. The geometry of the models correspond to the transversal view of the flume. The general boundary conditions considered are presented in Figure 4-9 where the green lines represent displacement boundary condition and the blue lines the flux boundary conditions. To reproduce the effect of the drainage element placed at the foot of the slope the boundary condition imposed considers that the outwards flow is zero if the liquid pressure is lower than the atmospheric pressure, but is higher than zero if the liquid pressure equals the atmospheric pressure (the soil reaches saturation). This boundary conditions avoids that the liquid pressure exceeds the atmospheric pressure but allowing that the liquid pressure be lower than the atmospheric pressure.

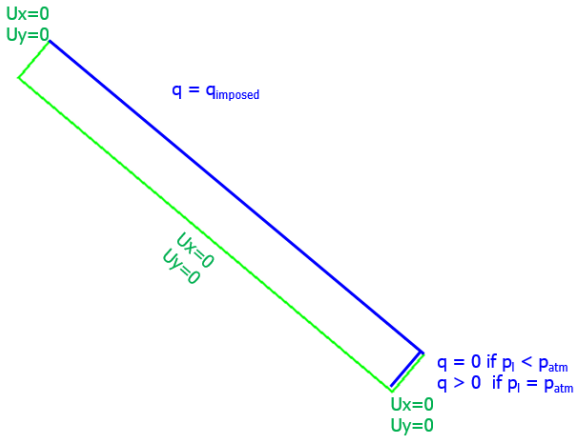

Figure 4-9 Flume test, boundary conditions.

4.2.1 Flume test D3.

This test was carried over a flume of 100 cm of length with an initial suction of 17.5 kPa and an initial porosity of 0.75. The complete description of the test is presented in section 2.1.2. In order to evaluate the response of the test a dense system of instrumentation was installed. Even so, not all the devices record appropriately the information. Figure 4-10 presents the devices of which the information is available.

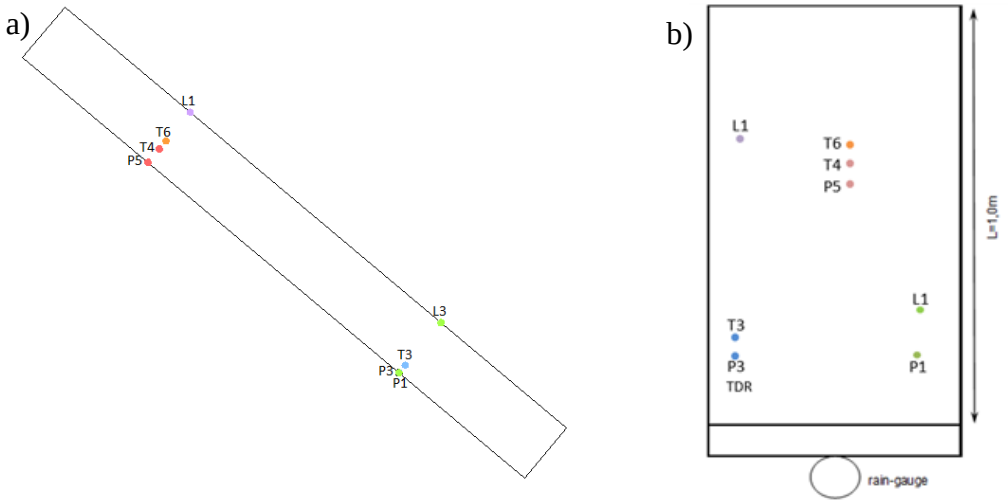

Figure 4-10 Geometry and location of instrumentation devices a) transversal section b) Planar view (T-minitensiometers P- liquid pressure transducers L- Laser sensors (settlements) TDR – Moisture profile)

The failure process experimented during this test consist in a mechanical failure due to a soaking process which produce the reduction of suction therefore the reaching of the yield surface. As was presented before the determination of the initial stress during the test is crucial for the failure calculation. To obtain these values or at least an initial stress situation appropriate to the process used for assembling the test. The method use for the creation of the sample was modelled. With this purpose a horizontal flume has been considered with a supposed initial porosity of 0.8. It is load with a vertical stress of 10 kPa then is unloaded. After this process the value of porosity obtained is equal to the value considered as initial for the soaking test. The stress condition over the flume after that the static load is removed has been considered as the initial stress condition for the soaking process. For the flume test D3 the stresses obtain are in the horizontal direction (σ_{xx}) 4.3 kPa, and for the vertical direction (σ_{xx}) 0.5 kPa, the value of preconsolidation pressure considered is 2.6 kPa.

Two different modelling conditions were considered to evaluate the response of this test a hydraulic model (H) and a hydro-mechanical coupling (HM). During the test the variation of suction within the flume test is recorded by 3 minitensiometers, 2 almost at the bottom of the flume (T3 and T4), but at different positions, and other at the middle of the flume (T6). Figure 4-11 presents the response obtain during the test compared with the behaviour obtain with the models. The evolution of suction is adequately simulated by the numerical models.

There are no many differences between the responses obtain with the hydraulic and the hydro-mechanical models. Furthermore, is interesting to observe that when infiltration starts the tensiometer located at the top of the flume (T6) registered an early and quick decrease in suction well-reproduced by the model. Tensiometers T3 and T4 respond also with a sharp decrease in suction but delayed for five minutes with respect to T6. This kind of response indicates the advance of a wetting front, well-captured by the model.

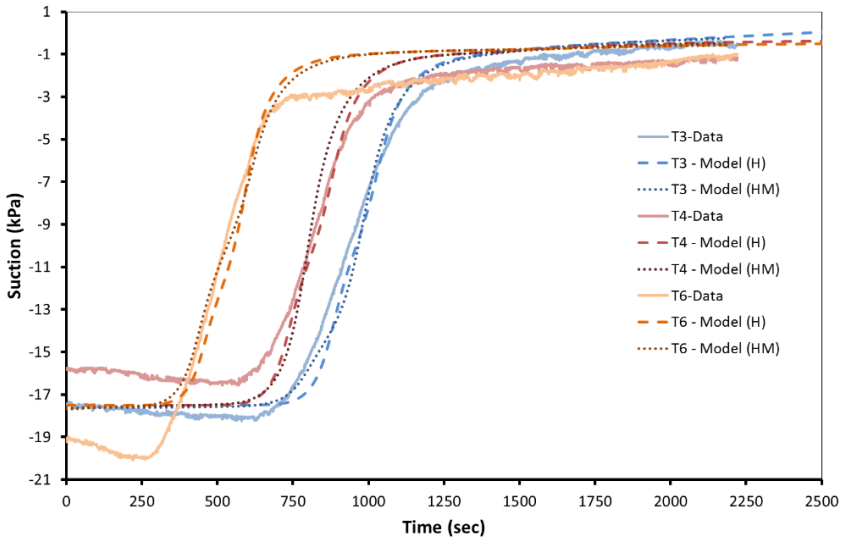

Figure 4-11 suction time evolution, test D3
(Continuous line: data recorded, dash line: hydraulic model, dot line: hydro-mechanical model)

The evolution of suction was complemented with liquid pressure transducers installed at the bottom of the flume which location are shown in Figure 4-10. For the geometry consider (transversal section) the liquid pressure transducers P1 and P3 are located at the same point. Figure 4-12 presents the response obtain. Although, the response observed during the test is not achieved with the model is interesting to observe the differences of the response between the 2 models. The values of liquid pressure are lower for the mechanical models, but the trend is very similar.

The measurements indicates that the liquid pressure starts to be higher than zero earlier in the liquid pressure transducers located closer to the top of the slope, but when the failure moment is close the values of liquid pressure are higher close to the foot of the slope. The latter phenomena is well reproduced by the model. This is caused to the infiltration characteristics of the test that close the foot of the slope the water accumulated include the vertical infiltration, due to the rainfall, and the transversal flow caused by the gravity and the impervious boundary condition of the bottom of the flume.

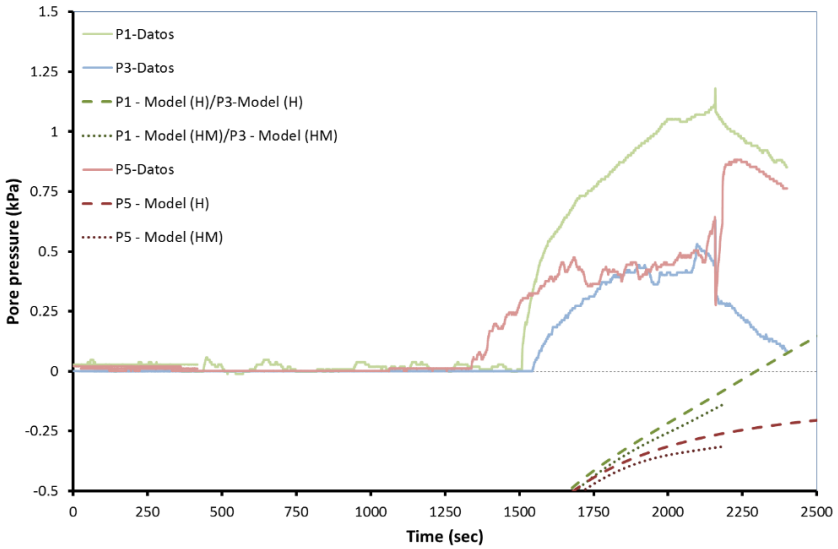

Figure 4-12 Liquid pressure time evolution, test D3
(Continuous line: data recorded, dash line: hydraulic model, dot line: hydro-mechanical model)

Another important response recorded during the test is the evolution of the water content. With this aim a profile of water content is obtain employing a new technique developed by Greco (2006). Several number of profiles are obtain in order to evidence its evolution with time. Figure 4-13 presents the response obtain with the hydraulic model.

It is considered that the value of water content at the bottom (z = 0cm) at the first profile (55 seconds) should be the initial water content. This is to say, the value of water content that correspond to a suction of 17.5 kPa. Is important to observed that the value obtain at this point with the model is very different to the data measured due to the water retention curve considered that is subjected to the differences observed between the results of test D3 and D4.

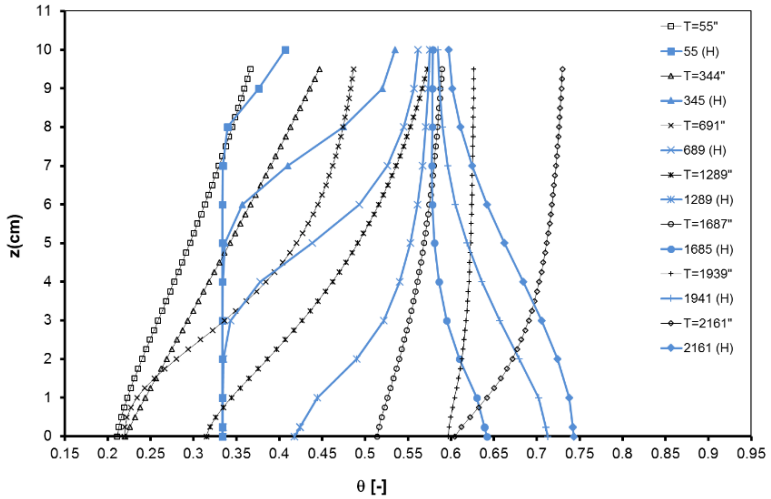

Figure 4-13 Volumetric water content profiles, hydraulic model, Test D3

To avoid this error the value considered is the increment in water content instead of the complete value as is shown in Figure 4-14 were the response obtain with the mechanical model is presented also. It is important to observed that until the time 1289 seconds the trend of the volumetric water content is well reproduced by the models in the other three profiles the value of water content at the bottom is well achieved but the rest of the profile is very different.

The measures indicated partial saturation of the upper part of the soil layer during the first 10 mins, followed by the deepening of the infiltration front that reaches layer bottom between 10 and 20 mins. From that time on, saturation increases more rapidly at the bottom than at the top of the sample and water content profiles travel to the right while becoming more vertical. This general pattern is consistent with the front-type advance of hydration evidenced by suction monitoring. After 32 mins, there is a new increase of water content at the top of the sample, of more difficult interpretation. Model captures qualitatively well the hydration pattern and also the quantitative change of water content at the base of soil layer.

The soaking process shown with the models generates an initial infiltration evidenced by higher values of water content at the top like what is expected. Once the water reaches the bottom and found an impervious boundary the water flows to the foot of the flume leading to higher values of water content at the bottom of the flume than in the top. Is also important to observe that when the mechanical process is considered the water content is higher. This is due to the reduction of the pores size due to the settlements which leads to higher values of water content.

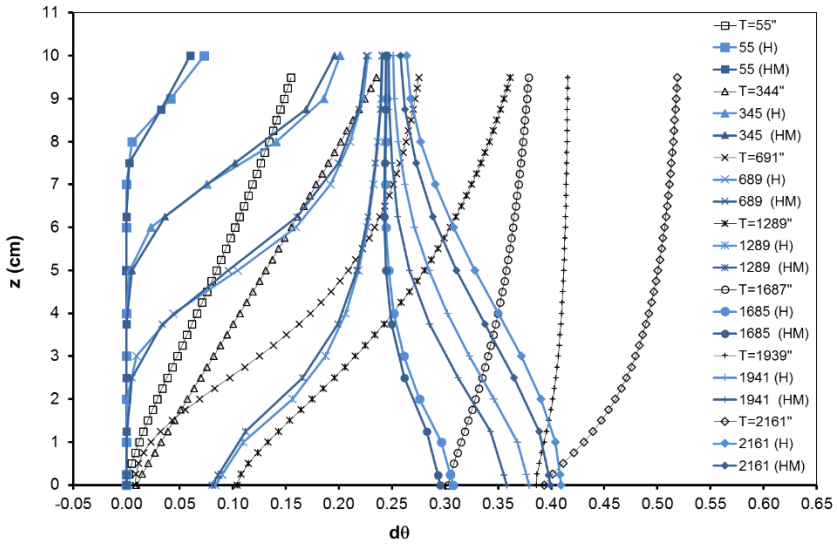

Figure 4-14 Delta of volumetric water content, test D3
(light blue: hydraulic model, dark blue: hydro-mechanical model)

Last but not least, the failure process is evidenced by the laser sensors transducers installed to obtain the settlements produced during the process. Two laser sensors are considered which location is presented in Figure 4-10. During the test the failure was registered at the 36 minutes (2160 seconds) with the model developed the failure was produced at the 2191 seconds when the model presented convergence problems. Just 30 seconds of difference with the measured data. Figure 4-15 presents the time evolution of the settlements recorded and achieved by the numerical model. Two additional points located at the foot of the flume and at the top (see Figure 4-16) were considered for the settlements time evolutions. With the numerical model an adequately value of final settlements registered during the test: 5 mm is achieved, even so, the trend obtain with the model is quite different of the one. With the model the collapse settlements are not well reproduced

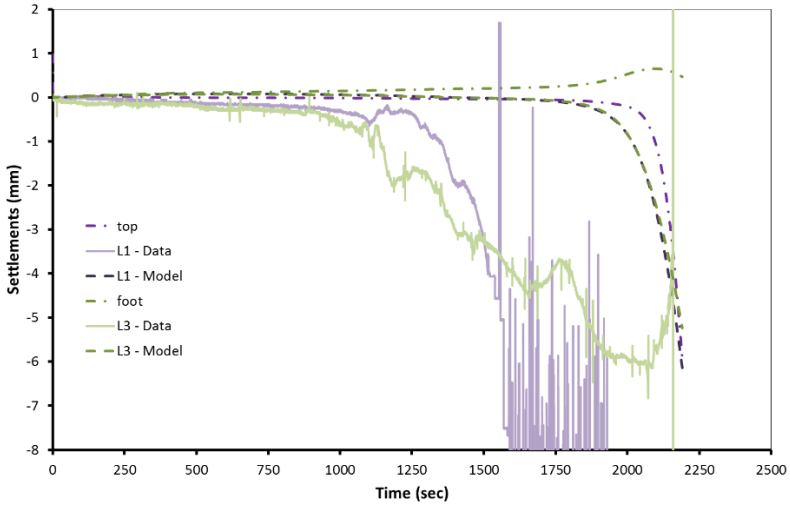

Figure 4-15 Settlements time evolution, test D3
(continuous line: data recorded, dash line: hydro-mechanical model)

Figure 4-16, shows the mesh deformed at the end of the failure process and the location of the additional points were the settlements are measured. The landslide failure is clearly evidenced. Further, is important to evaluate the evolution of the shear strains during the process presented in Figure 4-17 were is observed that by 1571 seconds the shear strains began to be developed. Finally by the 2191 seconds the shear band is complete developed generating the failure in the slope.

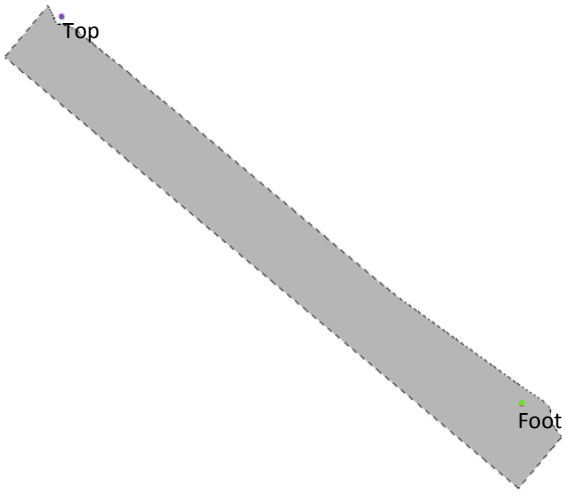

Figure 4-16 Mesh deformation at failure, test D3 (deformation factor: 2)

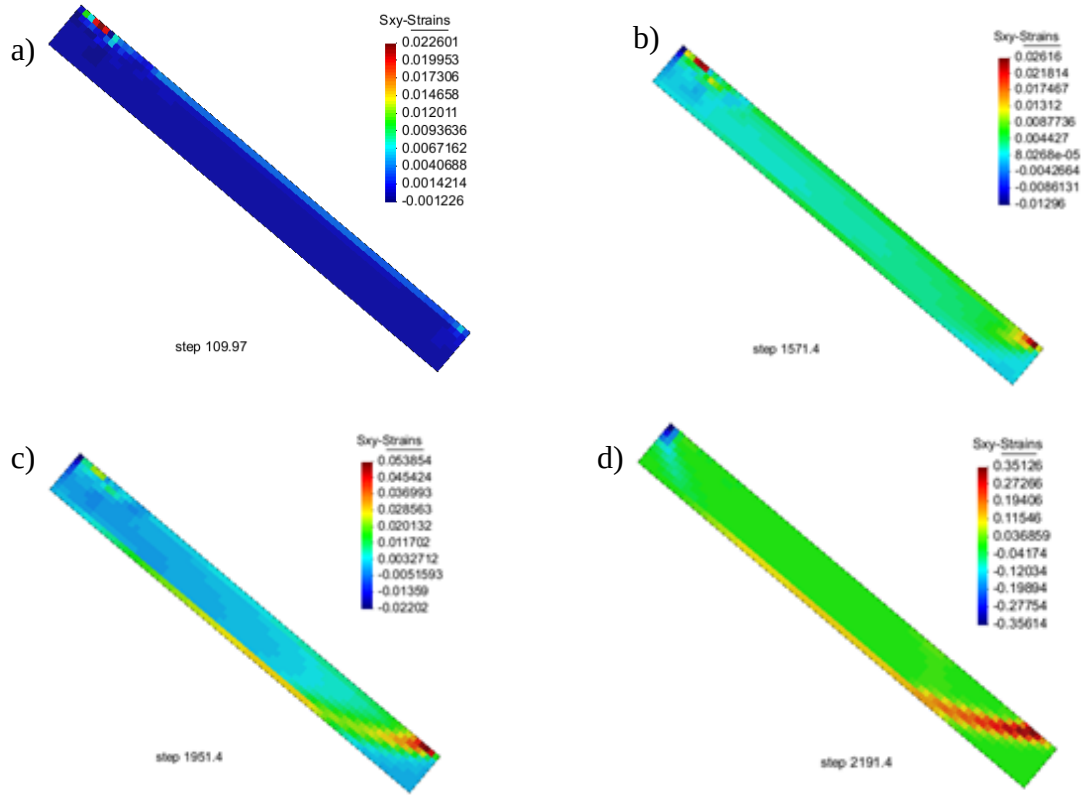

Figure 4-17 Shear strains evolution, test D3 a) time: 110 seconds b) time: 1571 seconds c) time: 1951 seconds d)time: 2191 seconds (failure)

4.2.2 Flume test D4.

The flume test D4 present an initial suction higher than the considered for the test D3 (43 kPa) this test is carried on over a flume of 1.20 m of length and 0.1 m of high. The complete description of this test in presented in section 2.12.

Like in test D3, many instrumentation devices were installed. But just a few devices record appropriately the information which location is presented in Figure 4-18. The transversal section presented in that figure represents the geometry considered for the model.

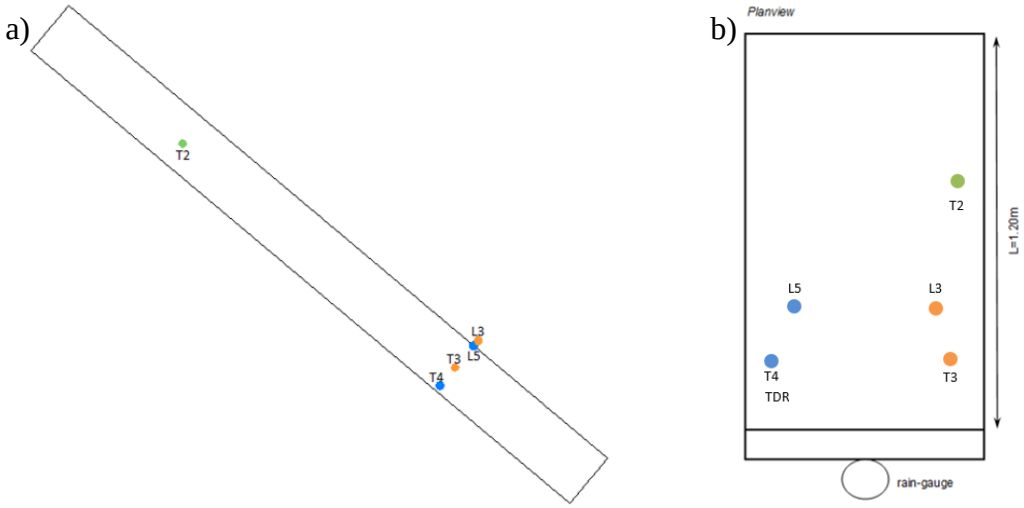

Figure 4-18 Geometry and location of instrumentation devices, test D4 a) transversal section b) Planar view (T-minitensiometers L- Laser sensors (settlements) TDR – Moisture profile)

The initial porosity of this test (0.76) is very similar to the porosity of test D3 (0.75) for this reason the stress condition that has been considered as the initial is the same for both test: 4.3 kPa in the horizontal direction (σ_{xx}), 0.5 kPa for the vertical direction (σ_{xx}), the preconsolidation pressure considered is 2.4 kPa.

On the other hand, the value of intrinsic permeability have been obtain with the kozeny´s relation presented in Figure 4-8. Even so, this value have been calibrated. The value of intrinsic permeability considered is 1.9 e-11. Taking into account these consideration the results obtain for this test are presented hereinafter.

For this test just 3 types of data are considered: evolution of suction, settlements and water content evolution. In the case, for the time evolution of suction three different points are evaluated: two at the middle of the flume (T2 and T3) and one at the bottom of the flume (T4). Identify with the letter T in Figure 4-18. In this case the effect of wetting front is evidenced also but with a delay of almost nine minutes. Figure 4-19 presents the comparison of the response obtain considering the mechanical coupling and without considering this coupling.

The characteristics of test D3 and Test D4 are very similar, especially the initial porosity and rainfall imposed, the important difference between this two tests is the initial mean suction. The value of the suction is a controlling parameter in the infiltration of water process. It controls the relative permeability which leads that the permeability of the test D3 (lower suction) be higher than the permeability of test D4 (higher suction). This feature could explicate why the delay between the measures realised in the middle and in the bottom in test D3 is lower than in test D4.

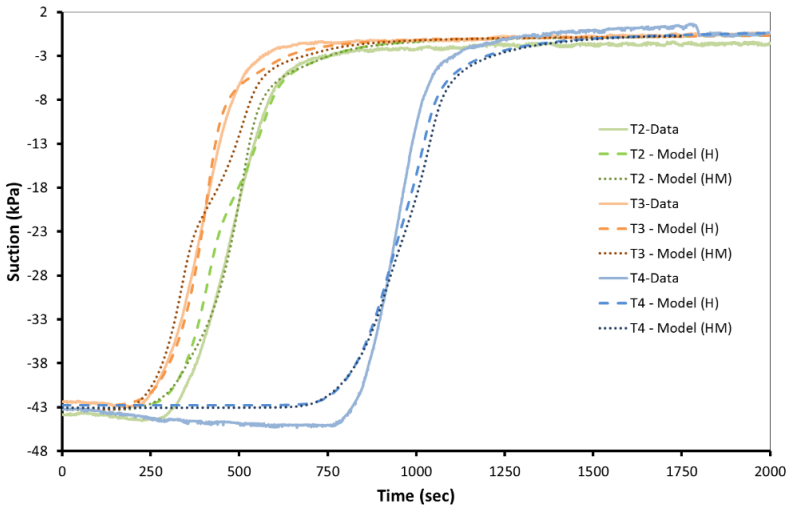

Figure 4-19 Time-evolution of suction for test D4
(Continuous line: data recorded, dash line: hydraulic model, dot line: hydro-mechanical model)

The volumetric water content profiles are obtain by the technique developed by Greco (2006). Like in the case of test D3, the initial value of water content is not determinate adequately by the model. For this reason, instead of evaluated the evolution of water content the delta of water content are evaluated and presented in Figure 4-20. It is observed that the trend obtain by the model until the time 1264 seconds is very similar to respond measured but, the measures data experiments a larger increases of water content since time 453 seconds. On the other hand, in this case the water content tends to a constant value at the top of the flume. Additionally just like in the case D3, when the mechanical process is coupled the water content is higher than when the problem considered is just the hydraulic process.

Like in the test D3 the response presented at the begging of the test consist in higher values of water content at the top of the flume but, at the end of the test the higher values of water content are at the bottom. This feature is due to once the soaking starts the infiltration is vertical but, when the water reaches the bottom it has to flow to the foot of the slope. This generates that at end of the test close to the foot of the slope the water flows to that point from 2 different directions. Is important to observe that for test D4 the change in the trend of the water content (more amount of water at the bottom than at the top) occurs at 1600 seconds while, for test D3 this process happens 300 seconds earlier (1300). This is attributed to the changes in relative permeability due to suction.

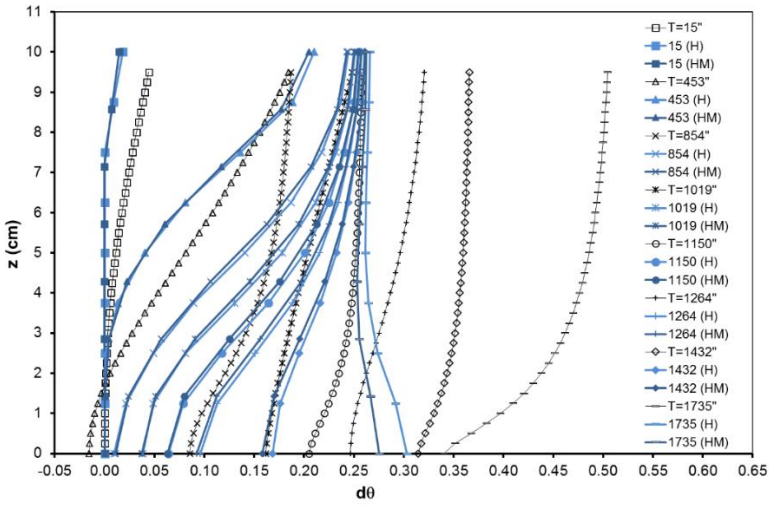

Figure 4-20 Delta of volumetric water content, test D4
(light blue: hydraulic model, dark blue: hydro-mechanical model)

The failure process is showed by the hydro-mechanical model. It is shown by the measurement of the settlements at the top of the flume test. For test D4 the devices considered are L3 and L5 this 2 devices are located at the same point if is considered just the transversal view (see Figure 4-18).

The response obtain with the model is compared with the behaviour measured in Figure 4-21 this data are complemented with two additional points located at the top and at the foot of the slope. The exactly position of this additional points is presented in Figure 4-22.

With the model the failure estimated is 1756 seconds (29.2 minutes) just 44 seconds earlier than what is reported in the test (1800 seconds) even so, the settlements behaviour suggest that the failure is around the 1750 seconds. With the model not just the time of failure is well predicted the value of the settlements achieved are similar to the values measured. Although, the failure obtain with the mechanical model is instantaneous for this reason the trend of settlements is different to the measured in the test. The collapse settlements are not appreciated.

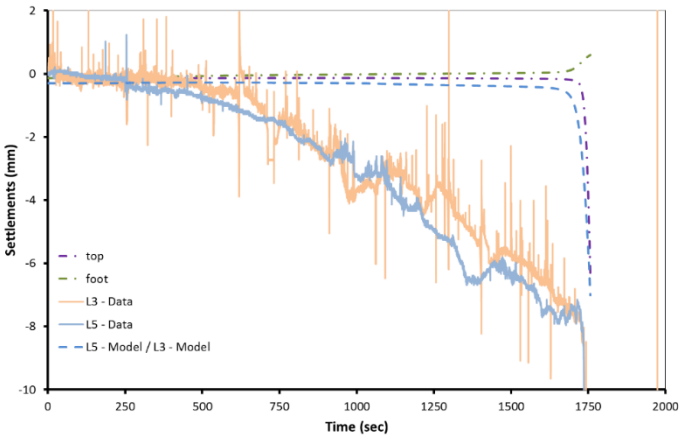

Figure 4-21 Settlements time evolution Test D4
(continuous line: data recorded, dash line: hydro-mechanical model)

Figure 4-22 present the mesh deformed after the test where is observed the crown and the foot of the landslide generated by the failure and slide of the material. Due to the reduction in suction caused by the soaking process. As the settlements registered are around the 8 mm (8% of the height) the deformation is larger by a factor of 2, in order to observe better the deformations generated.

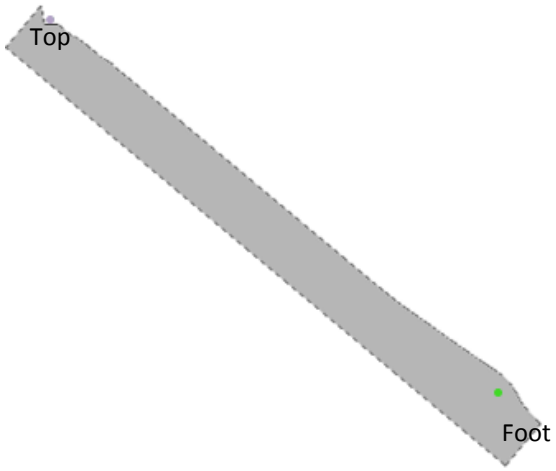

Figure 4-22 Mesh deformation at failure, test D3 (deformation factor: 2)

Equally important is the time evolution of the shear strains presented in Figure 4-23 which shows the distribution of the shear strains for 4 different moments during the test D4. It is observed that by the time 1570 seconds the generation of the shear band begin. It is evidenced by a concentration of shear strains at the foot of the slide and the failure is guide by the bottom of the flume. Finally the crown crack is developed.

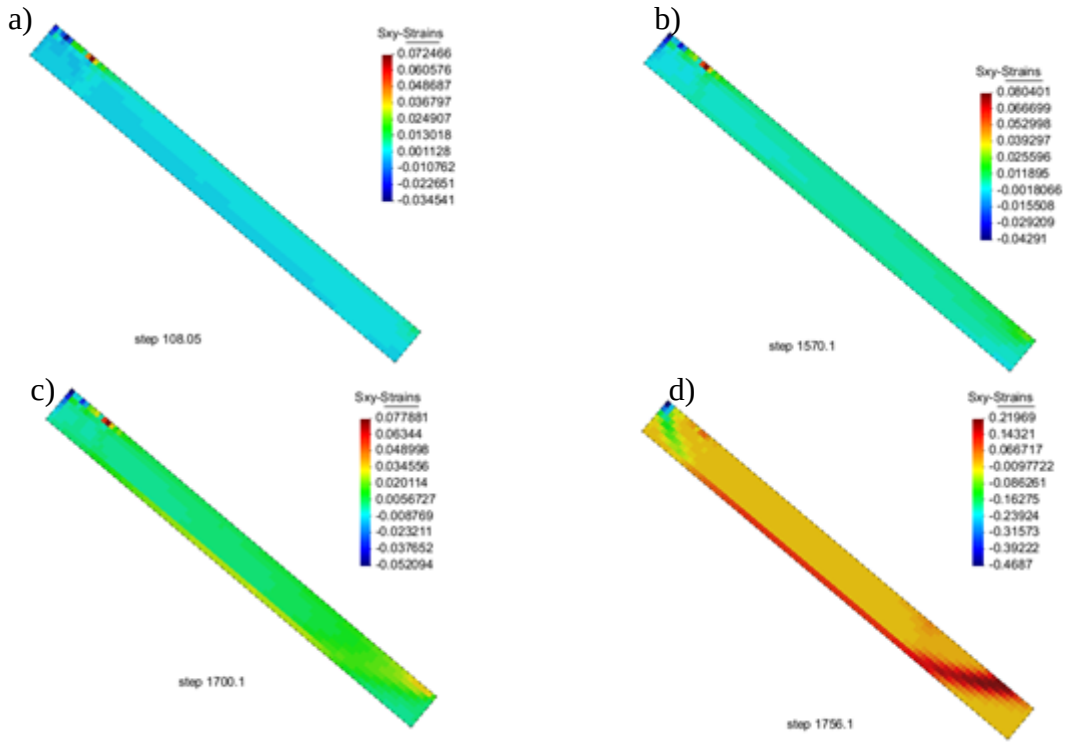

Figure 4-23 Shear strains evolution, test D4 a) time: 108 seconds b) time: 1570 seconds c) time: 1700 seconds d)Time: 1756 seconds (failure)

4.2.3 Flume test C4.

The principal objective of the benchmark exercise was the prediction of the behaviour of a flume test with specific characteristics of: geometry, porosity, initial suction and rainfall. Using the information of test D3 and D4, and the laboratory test realized. The test to be predicted is the test C4, which principal characteristics are listed in Table 4-4.

Table 4-4 Characteristics of test C4

Test	Soil Thickness (cm)	Slope Length (cm)	Initial Porosity n_0	Rainfall intensity (mm/h)	Initial mean suction (kPa)
C4	10	110	0.65	60	52

The information that should be presented was:

- Time of slope failure
- Time evolution of soil suction, at locations were the minitensiometers were installed, T in Figure 4-24
- Soil surface settlements at the location were the laser sensors transducers were installed, L in Figure 4-24
- Pore water pressure at the bottom, at locations were the pressure transducers were installed, P in Figure 4-24

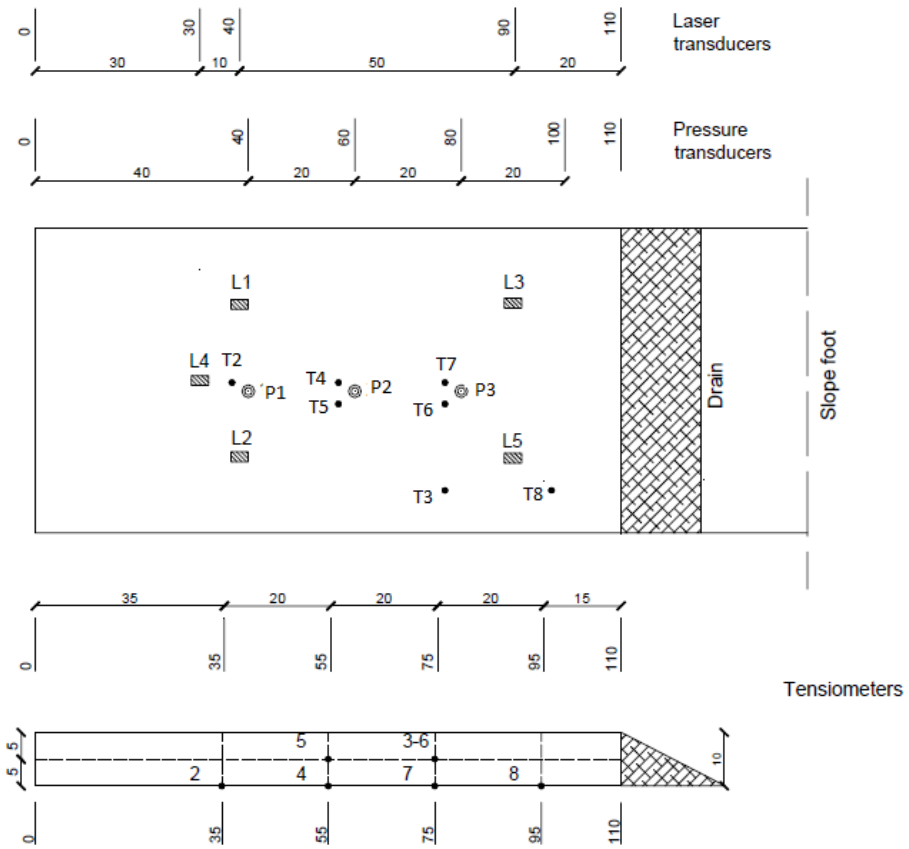

Figure 4-24 Geometry and location of instrumentation devices for test C4, from information of Round Robin contest

The modelling process of this test is the same employed for the test D3 and D4. Two different model conditions are considered: a hydraulic model and a hydro-mechanical model essentially to evaluate the difference in the response obtain with this two conditions. The geometry considered for the model is presented in Figure 4-25. Just like in the two cases showed earlier the geometry considered is a transversal section of the flume which leads that in some cases two instrumental devices be located at the same point.

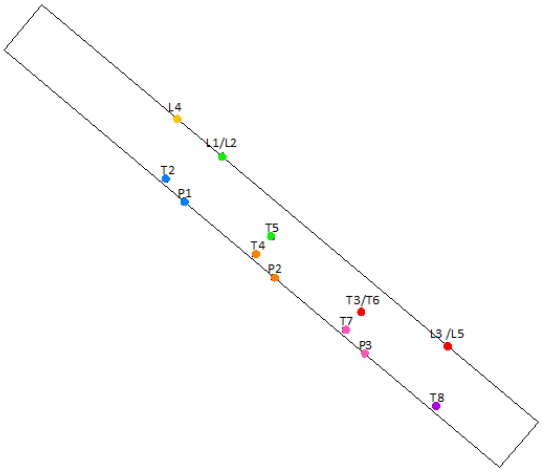

Figure 4-25 Geometry of the model (transversal section) and location of instrumentation devices, test D4 (T-minitensiometers L- Laser sensors (settlements) TDR – Moisture profile)

The initial porosity of test C4 (0.65) lower than the porosity considered for test D3 and D4. This change will generate important differences in the hydraulic and mechanical parameters. For the hydraulic conditions the value of intrinsic permeability should be corrected with the porosity. This variation is presented by the kozeny´s law shown in Figure 4-8. The value of intrinsic permeability consider is 5.9 e-12 m^2.

Further, for the mechanical behaviour the condition of initial stress has to be different. Inasmuch as the value of the porosity is lower a high static load will be necessary during the sample preparation to achieve the value of porosity desired. Considering an initial porosity of 0.77 the static stress needed is 50 kPa which leads a stress condition of: 5.5 kPa at the horizontal direction (σ_{xx}), and 0.4 kPa for the vertical direction (σ_{xx}). Additionally, the value of preconsolidation pressure considered is 3.2 kPa

Olivares & Tommasi (2008) present the response for different flume test. One of the cases reported present similar characteristics of the test C4. For this reason the response obtain with the model will be compared with the performance presented in this paper. Taking into account that the precise location of the devices is not reported. The response registered is presented in terms of soil suction and settlements.

Figure 4-26 presents the time evolution of soil suction. The most important characteristic observed is the effect of advance of wetting from that generates that the superficial devices (T5, T3 and T6) suffer a decrease in suction earlier than the deeper tensiometers (T2, T4, T7 and T8). The same feature is observed in the flume test response registered in Olivares & Tommasi (2008). On the other hand when the mechanical coupling is considered the behaviour observed is very similar to the performance of the hydraulic problem but, for the hydraulic problem the values of suction are slightly high.

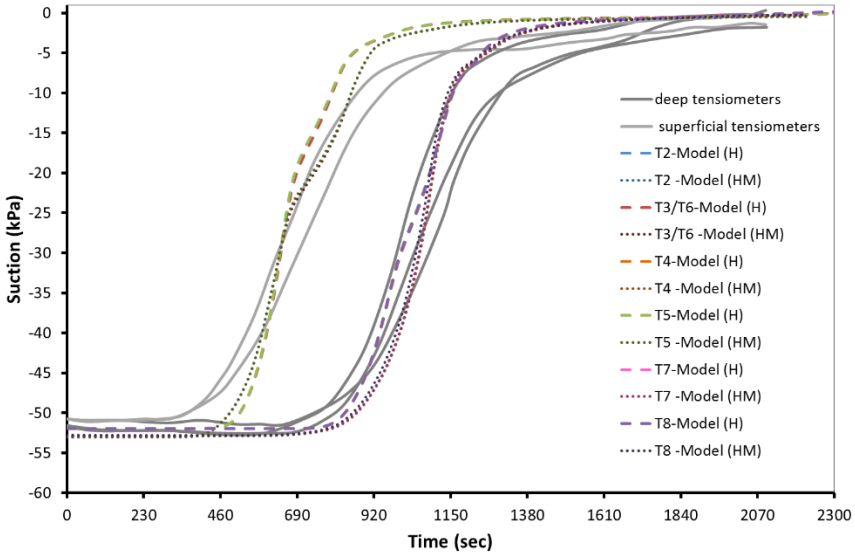

Figure 4-26 Time-evolution of suction for test C4, from Olivares & Tommasi (2008) (dash line: hydraulic model, dot line: hydro-mechanical model)

The time of failure of the slide and the settlements are obtain with the hydro-mechanical coupled problem. The model present convergence problems at the time 2215 seconds. It is considered that this convergence problems are attributed to high values of strain, that is to say, the failure of the slide. For this reason the time of failure is 2215 seconds (about 37 minutes). Conversely of the response observed in the test D3 and D4, the performance report by Olivares & Tommasi (2008) for test C4 consider settlements of less than 1mm until 2000 seconds.

The response achieved by the model is very similar to the behaviour registered but, at the failure the flume suffer settlements of almost 8 mm as is presented in Figure 4-27. In this case two additional points are evaluated also one at the foot of the landslide, and other at the top of the slide. Is important to mention this predictions of failure time and the evolution of soil suction, were designated as winner of the class A benchmark on hydrological modelling of slopes at the Italian workshop on landslides, 23rd October 2013.

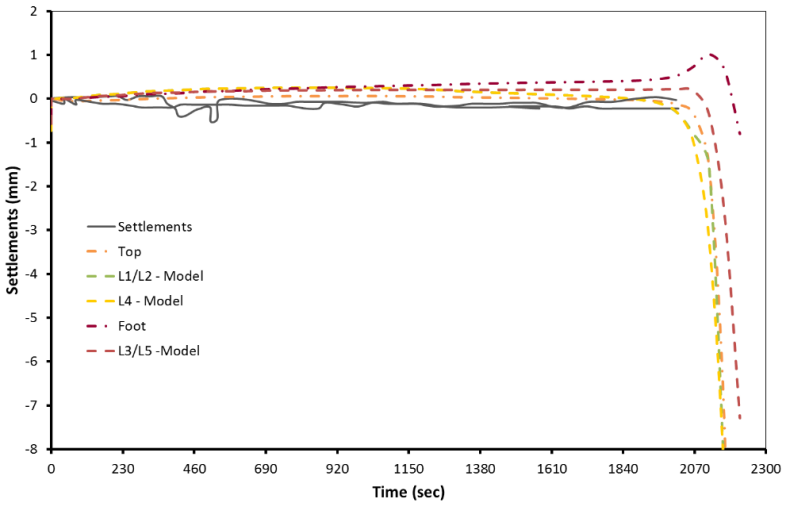

Figure 4-27 Settlements time evolution, test C4, from Olivares & Tommasi (2008)

The evolution of liquid pressure at the bottom is not reported by Olivares & Tommasi (2008). Even so, the response obtain by the models is shown in Figure 4-28. Observed that for this test the liquid pressure reaches positive values at 2100 seconds in the hydraulic model and in all the points evaluated the response obtain with the hydro-mechanical model present lower values of liquid pressure than the presented in the hydraulic model.

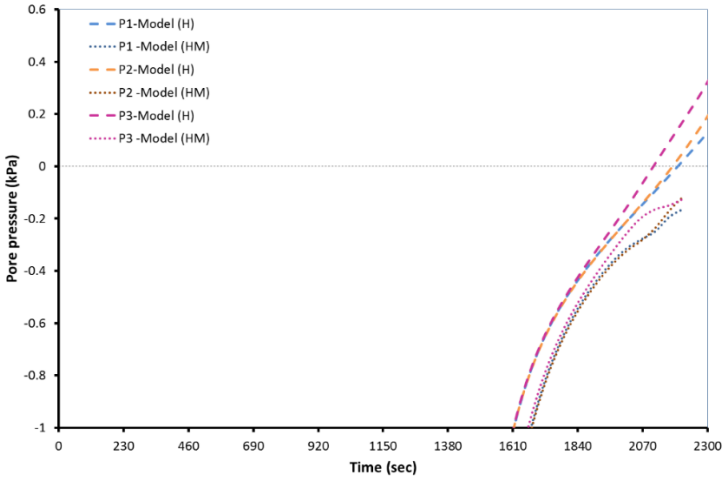

Figure 4-28 Liquid pressure time evolution, test C4
(Continuous line: data recorded, dash line: hydraulic model, dot line: hydro-mechanical model)

Furthermore, the failure process presented by this test is very similar to the response presented in test D3 and D4. Figure 4-29 show the evolution of shear strains similarly to the cases presented before the failure is characterized by a shear band limitated by the bottom of the flume test. The development of this shear band is observed from time 1355 where the shear strains concentrate at the foot of the slope. Figure 4-29d present the shear strains developed at the failure over the deformed mesh.

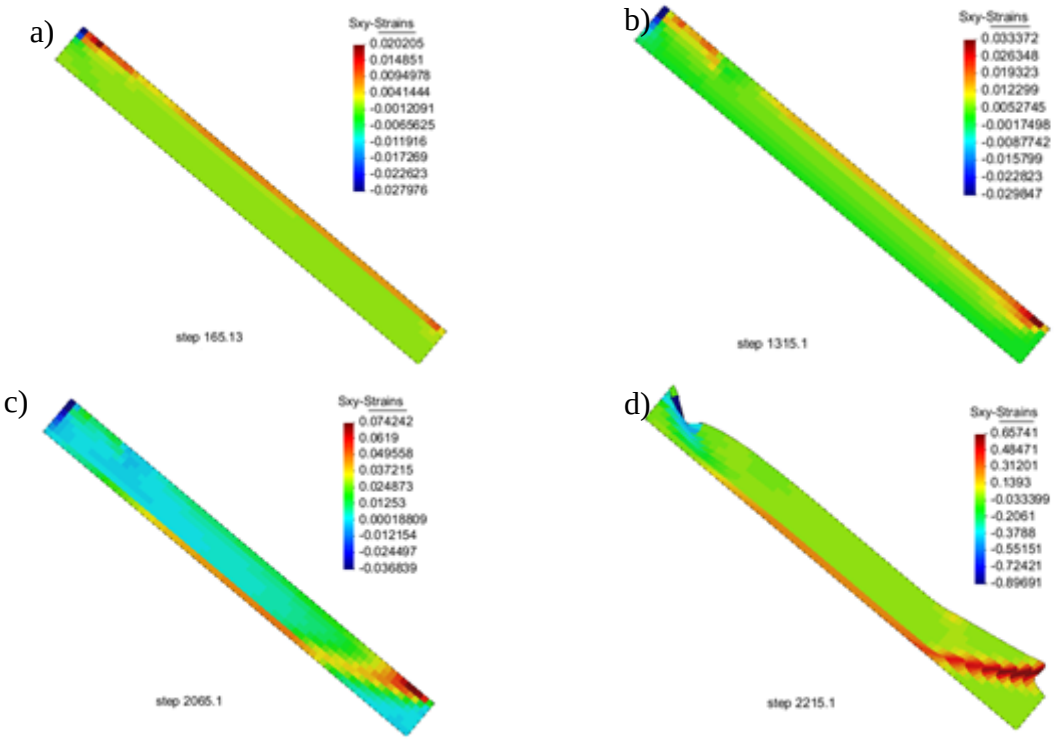

Figure 4-29 Shear strains evolution, test C4 a) time: 165 seconds b) time: 1315 seconds c) time: 2066 seconds d) time 2215 seconds (deformed mesh, factor:2)

4.3 REAL SLOPE.

The principal aim of the study that developed of the flume test is to obtain better information about superficial landslides triggered by rainfall. In order to obtain better explanations of the rain-triggered landslides. The analysis is focus in the slopes of Cervinara, southern of Italy.This zone is very susceptible to rainfall induced landslides. (Olivares et al. 2009)

With this purpose, the slope of Cervinara located in the mountainous area. 50km northwest of Naples, southern Italy has been equipped with an automatic instrumentation station to record the evolution of water content and liquid pressure every two hours since august 2009. This system is complemented with a rainfall gauge. The characteristics of the slope and the field monitoring system are presented in section 2.1.3

After two years of field monitoring Comegna et al. (2013) concluded that: the slope present very little surface runoff, in general the soil is always far from saturation (the volumetric water content rarely exceed 0.4) and that the aquifer plays an important role in the evolution of the soil suction at all depths. Every year from May on the level in the aquifer decrease generating an increase in the soil suction in the superior layers. This feature is evidenced in the fact that the suction increasing trend in the deepest tensiometers is steeper than above.

In fact, Greco et al. (2013) present the evolution of water potential which evidences that during the summer the vertical water flux is always directed downward toward the bed rock. Even when not rainfall is registered. This response is very typical of the mountains of southern Apennines during the dry seasons. Unfortunately from the variations of water level within the aquifer not precise information is available.

In general, the soil stratification of this site can be defined by three layers: the first 1.5 meters are constituted by a mixture of pumices and ashes, above a layer of 1.0 m tick of pumices laying upon the fractured limestone. One of the most important features of the monitoring system is that in some cases values of water content and suction are measures at the same depth. With the aim to define the water retention curve for each layer considered. This pairs of values are obtain form the devices located at 0.6 m and 1.0 m placed in the layer of pumices and ashes and the devices at 1.7 m depth at layer of ashes.

Furthermore, the response appreciated with this devices suggest that the shape of the water retention curve (WRC) that better define the in situ behaviour is a double porosity WRC. Like what happens with the laboratory and flume test. Moreover, this WRC is different to the one define with the laboratory test and with the flume test. Due to the differences in the conditions of flux generated by the characteristics of the test or/and sample preparation. Figure 4-30 present the water retention curve considered for the pumices and the ashes. It is observed that like was presented in section 2.1.3 the data that correspond to higher values of suction for the device located at 1.0 depth present an inconsistent behaviour.

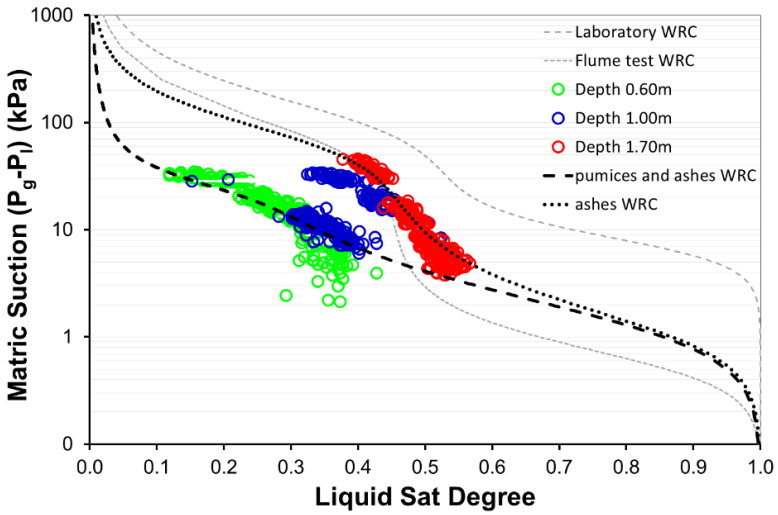

Figure 4-30 Water retention curve for field monitoring exercise.

As has been mentioned earlier, in this region the rainfall-triggered landslides are very common. The failure is caused by the decrease of water suction due to the infiltration of rainfall. The hydraulic characteristics of the material and the rainfall conditions play an important role in this process even though these are not the only conditions that control the water infiltration in the material. The parameters that govern the evaporation, the flux of energy and the flux of gas, are very important also. Inasmuch as, they controlled the amount of water available to infiltrate across the soil surface. For this reason, in order to model the response of the soil suction and volumetric water content the climatic actions is necessary to consider a Thermo-Hydraulic coupling.

The rainfall and temperature available correspond to year 2011. On the other hand the information of tensiometers and water content presented correspond to the first seven months of this year. This information is shown in section 2.1.3. The aim of the Thermo-Hydraulic model considered is to well reproduce the behaviour of liquid pressure and water content within the slope based on the information available.

The geometry considered for the numerical model consist in a 2D column with 3 m width and 5 m height which leads to consider 2.5 m of the limestone in the model. Additionally the slope

is covered by a wood which present some permanent vegetation and other seasonal vegetation that become denser from May to September. Greco et al. (2013) report that the roots of this plants present the maximum density in the first 0.4 m but, the presence of roots can reach 1.5 m depth, in this case the depth of root considered is 0.4 m. Figure 4-31 presents the geometry considered for the model.

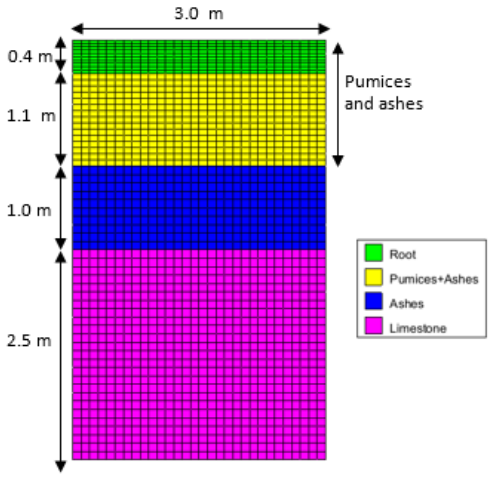

Figure 4-31 Geometry of model for the field slope

According to Rahardjo & Lee (2005) and Leroueil (2001) the conditions of pore pressure and saturation degree before the rainfall event determinate the hydraulic conductivity and the quantity of water required to the soil reaches saturation. Even though the determination of these values is very complex. They depend on the antecedent hydraulic condition.

For this reason, although the profile of liquid pressure for first day of simulation (01/01/2011) is known (see Figure 4-33 a) Initial conditions b) boundary conditionsan equilibrium time is considered, that is to say, several number of years are modelled with the same atmospheric conditions until the response is stable. Figure 4-32 present the results for a 1095 days (3 years) equilibrium time modelling were the atmospheric conditions are the same for each year. Is important to observe that for year 2 and 3 the response is equal for this reason it is considered that at this moment the response is stable.

On the other hand, Figure 4-33 present the boundary conditions considered for the model and the initial conditions of suction. The boundary conditions represent the atmospheric actions over the slope and the effect of the root zone. Additionally a boundary condition considered at the bottom allows the flow of the water across this boundary. Further, considering in this boundary a special liquid pressure boundary condition the effect of the decreasing in water level within the aquifer can be included.

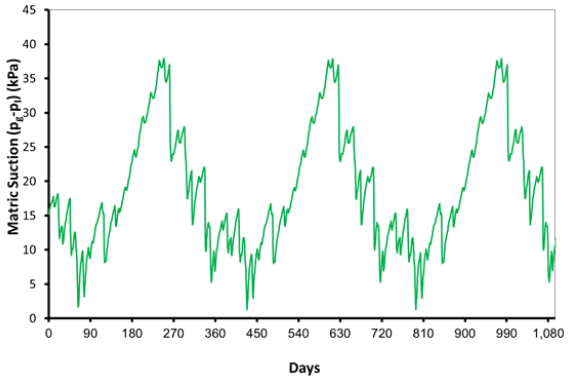

Figure 4-32 equilibrium time (0.60 m depth)

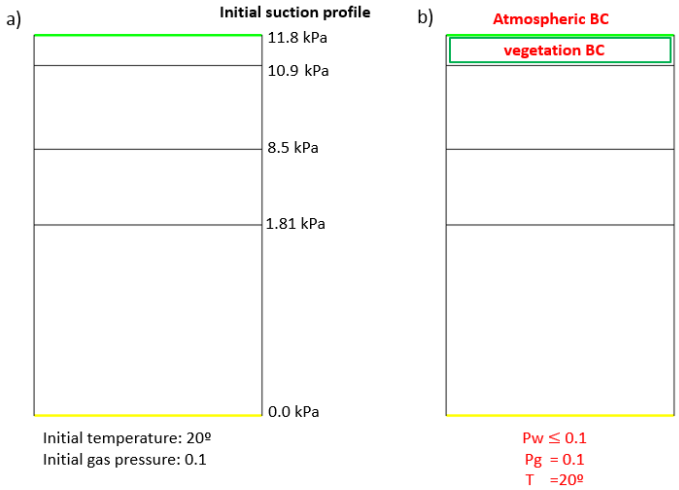

Figure 4-33 a) Initial conditions b) boundary conditions

The pyroclastic materials (pumices and ashes) found in Cervinara region are characterized by high values of porosity between 0.70 and 0.75. In this case the value of porosity considered is 0.70. In order to reduce the unknown parameters it had been considered that the thermo – hydraulic parameters for the pumices and the ashes will be the same. Changing just the WRC because this is the only information available that make differences between this two layers.

The value of intrinsic permeability was calibrated. For the superior layers (pyroclastic soil) the value considered is 5e-13 m^2 and for the limestone: 4.5 e- 14 m^2. The water retention curve used for the limestone was the same than for the pumices and the value of porosity for this material is 0.25 (Typical value for fractured rocks). Table 4-5 Thermo-Hydraulic parameters.presents a summary of the thermo-hydraulic parameters considered

Table 4-5 Thermo-Hydraulic parameters.

Property		Pumices and ashes	Ashes	Limestone
Porosity	ϕ	0.7	0.7	0.25
Intrinsic permeability Darcy´s law	K (m^2)	5e-13	5e-13	5e-13
Liq. phase rel. permeability Generalized power function	A	1	1	1
	λ_{rp}	3	3	3
Water retention curve Double porosity WRC	P_{0M} (kPa)	1.4	1.2	1.2
	λ_M	0.45	0.5	0.5
	P_{0m} (kPa)	25	75	75
	λ_m	0.75	0.6	0.6
	w	0.18	0.43	0.43
	S_{rl}	0	0	0
	S_{ls}	1	1	1
Diffusive flux of vapour Fick´s law	$D\left({}^{m^2 P_a}/_{sK^n}\right)$	5.90e-6	5.90e-6	5.90e-6
	τ	1	1	1
	n	2.3	2.3	2.3
Conductive flux of heat Fourier´s law	$\lambda_{sat}\left({}^{Wm}/_{k}\right)$	1.2	2.3	2.3
	$\lambda_{dry}\left({}^{Wm}/_{k}\right)$	1.2	2.3	2.3

Besides the thermo-hydraulic characteristics of the material, the evolution of liquid pressure within the soil is governed by the parameters that control the ground atmosphere interface and the evapotranspiration (vegetation parameters) presented in section 3.3.

The characteristics of evaporation and evapotranspiration are controlled mostly by the values of the aerodynamic resistance (r_a) and vegetation fraction (veg), as is presented in section 3.3. Noilhan & Planton (1989) shown that the value of veg fraction for a forest is 0.99. On the other hand the parameter ra depends on: the screen height (z_a), the ground surface of roughness (z_0) and the wind velocity. The value of ground surface roughness depends on the height of the vegetation. Greco et al. (2013) report that at the slope the vegetation reaches 15 m leading a value of z_0 equal to 0.7. The value of z_a has to be calibrated. Additionally Greco et al. (2013) and Comegna et al. (2013) present the typical value of some of the parameters that control evaporation and evapotranspiration.

The values of temperature and rainfall should be completed with the wind velocity, index cloud and air relative humidity values in order to have the hydrological conditions complete, the radiation had been calculated based with the temperature and location, as is shown in section 3.3.3.

The missing information had been obtain by the average annual information recorded in the hydrological station of the Capodichino Airport (Naples international airport) (WeatherSpark 2014). It is reported a mean wind velocity of 2m/s, a mean relative humidity of 0.7. Finally the value mean index cloud present an important variation during the summer, the mean value observed is 0.5, but for the summer months this value decrees until a value of 0.3. Table 4-6 present the summary of meteorological, vegetation and ground-atmosphere interface parameters

Table 4-6 meteorological, vegetation and ground-atmosphere interface parameters

Meteorological data			**Ground/atmosphere interface**			**Vegetation**		
Wind velocity (m/s)	v_a	2	Albedo	A_l	0.25	Vegetation fraction	veg	0.99
Air relative humidity	H_r	0.7	Roughness coefficient	z_0	0.7	Limit global radiation $(J/_{sm^2})$	R_{gl}	30
Index cloud	I_n	0.5	Screen height	z_a	2.2	Min surface resistance (s/m)	r_{smin}	400
Summer index cloud	I_n	0.3	Leakage coefficient	No ponding condition	-1e6	Max surface resistance (s/m)	r_{smax}	2800
						Leaf area index (m^2/m^2)	LAI	2.5
						Wilting point	s_l^w	0.05
						Field capacity	s_l^{fc}	0.33
						Anaerobiosis point	s_l^a	0.98

The aerodynamic resistance is probably the most controlling parameter in the calculation of evaporation, see Eq. 3-12 and depends in characteristics of the vegetation of the place and on the hydrological characteristics of the site. Most important the value depends in height to which the absolute air humidity and wind velocity are measured. In this case this data is not available. Moreover, the wind velocity and air humidity not are measured at the location of study. For this reason a sensibility analysis has been realized to evaluate the effect of this parameter. Figure 4-34 present the effect of the aerodynamic resistance. It is important to observe that when the

value of r_a is higher the evaporation is lower which leads to higher values of suctions. Especially during the summer. Additionally this effect is higher close to the surface but even so at 1.4 m the effect can be appreciated. The value used for the model is $r_a = 4$.

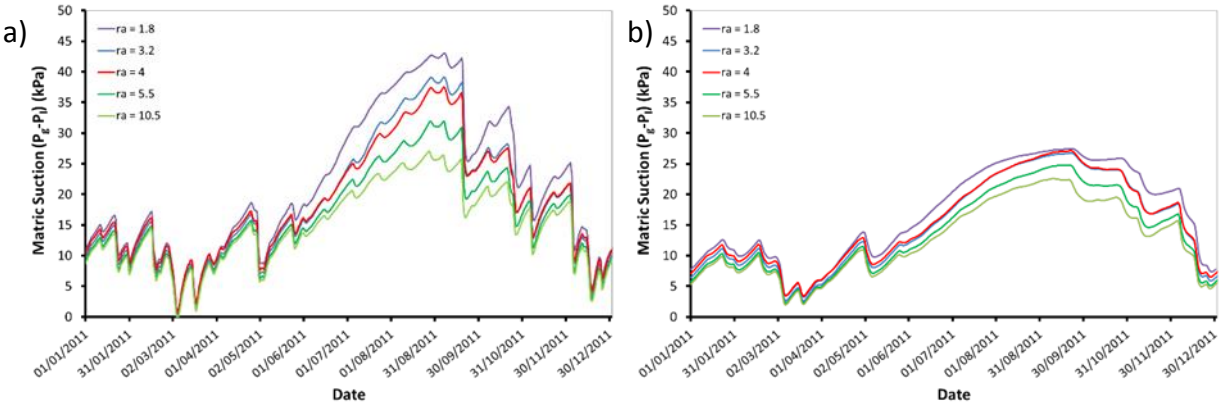

Figure 4-34 Effect of r_a a) 0.60 m depth b) 1.40 m depth

Apart from the climatic actions, the slope is subjected to the influence of an aquifer located in the limestone which decreases in water level during the summer plays an important role in the hydraulic conditions of the material above this rock. Comegna et al. (2013) present the importance of taking into account the evolution of the aquifer water level within the hydrological model for this slope.

The behaviour of this aquifer is not well known, for this reason there is not information available of the evolution of the water level within the aquifer. But is well known that the decreases of this water level causes the increment in liquid suction in the pyroclastic materials. In order to reproduce the effect that the aquifer present in the soil a special boundary condition is implemented at the bottom of the model which consist in a ramp of suction. This will lead that during the summer the flow will be mostly downward, regardless the atmospheric conditions.

Comegna et al. (2013) consider that the effect of this aquifer begging in May. Additionally that this aquifer could be modelled by a linear reservoir model with a time constant around 60 to 90 days. This parameter suggest the velocity for the drainage in this case for the reduction in the aquifer water level. Considering this. The boundary condition considerer to simulate the effect of the aquifer consist in a ramp of suction that begging at the end of May. At this time the value of liquid pressure begging to decrease over 60 days until a value of 0 kPa. This value is constant until the end of the summer. At the end of September the value of liquid pressure increased over 60 days until recover the initial value (0.1 kPa)

The liquid pressure boundary conditions considered at the bottom of the model, with the aim to reproduce the effect of the aquifer is presented in Figure 4-35. In Figure 4-37 Results of back-analysis for the data provided a) 0.60 m depth b) 1.0 m depth c) 1.40 m depth d) 1.70 m depthis appreciated the importance to consider the effect of the aquifer. Without this boundary conditions is not possible to achieve the response observed by the instrumentation system.

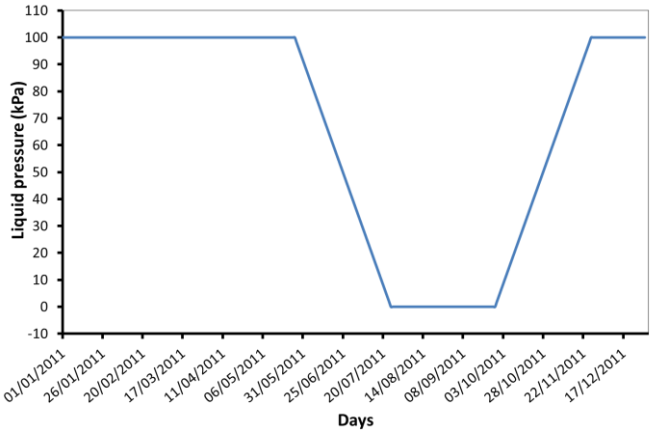

Figure 4-35 Liquid pressure boundary condition

Taking into account all the considerations presented above. The model is realized including the concept of equilibrium time and the effect of the aquifer coupled with the atmospheric boundary condition presented in section 3.3. In order to obtain a better response, but without consuming many calculation time five years are considered to obtain the stationary response. The first three years without considering the effect of the aquifer. Figure 4-36 present the response of the time modelling considered. It is important to observe the effect of the aquifer that generates higher values of suction.

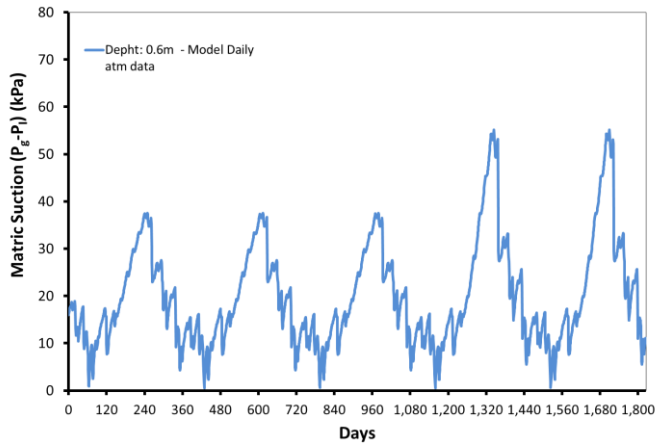

Figure 4-36 Complete time modelling.

Figure 4-37 present the results obtain with the model for the back analysis time provided. In all the depths considered the model reproduce adequately the behaviour measured. Though, the lower peaks of suction are not well reproduce by the model.

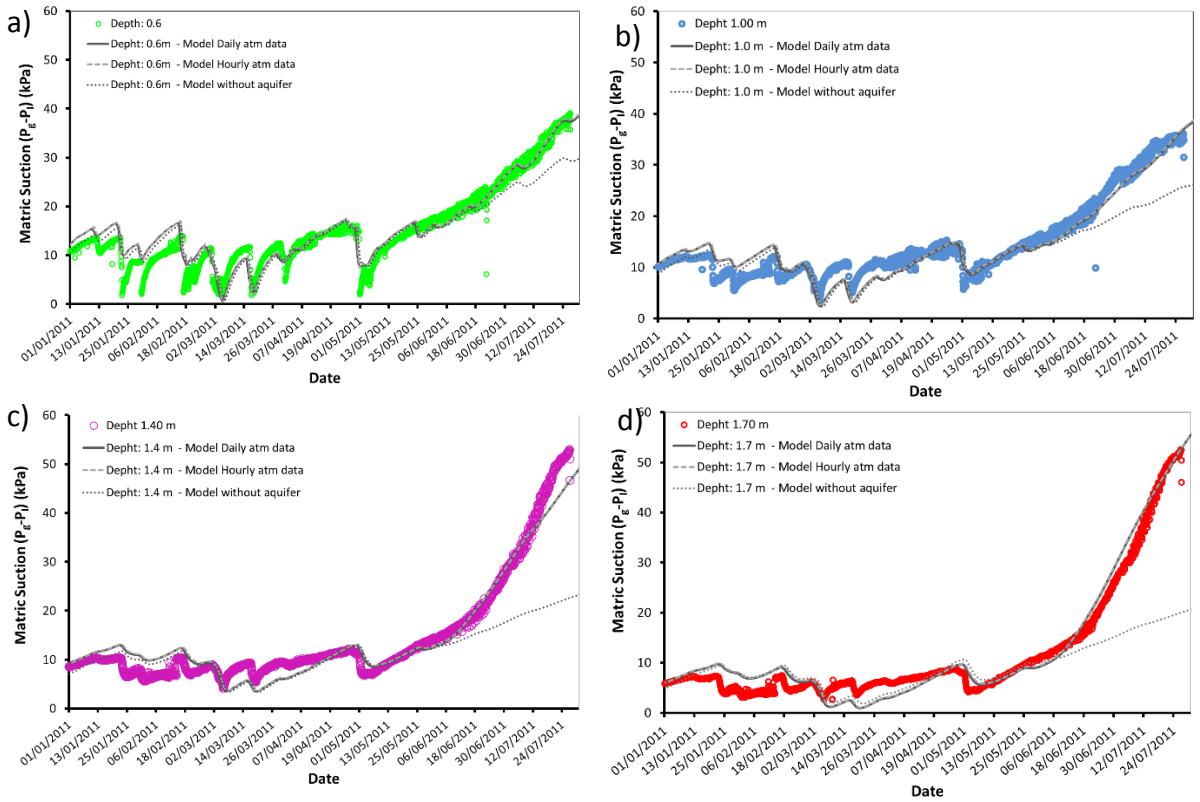

Figure 4-37 Results of back-analysis for the data provided a) 0.60 m depth b) 1.0 m depth c) 1.40 m depth d) 1.70 m depth
(continuous line: model used, with daily atmospheric data, dash line: With hourly atmospheric data dot line: model without the aquifer effect)

Even thought, the rain gauge located at site present record the data each hour. The atmospheric data considered for the modelling are the daily data with the aim to reduce the calculation time. Figure 4-37 presents the comparison between the results obtain with the daily atmospheric data and the hourly atmospheric data, is evidenced that the approach realized do not represent any error in the simulation.

Finally, Figure 4-38 presents the response of the liquid pressure expected for year 2011 with the model presented and Figure 4-39 represent the evolution of water content. It is observed that as was expected the suction reaches its maximum values at the end of the summer. The volumetric water content evolution obtain with the model fits with the data measured in the soil. Although, the volumetric water content at depth 0.3 is slightly lower than the values measured probably because at this depth the roots of the vegetation are very dense. In general the trend in all depths is adequately reproduced. On the other hand, the departure observed for the last two months in Figure 4-39C is to be related to the discrepancy existing between the suction-water content relationship measured from January to May 2011 (blue points close to the green ones in Figure 4-30) and after this period (blue points close to red ones). The causes for such a sudden jump in time of the instrumentation results have to be further investigated.

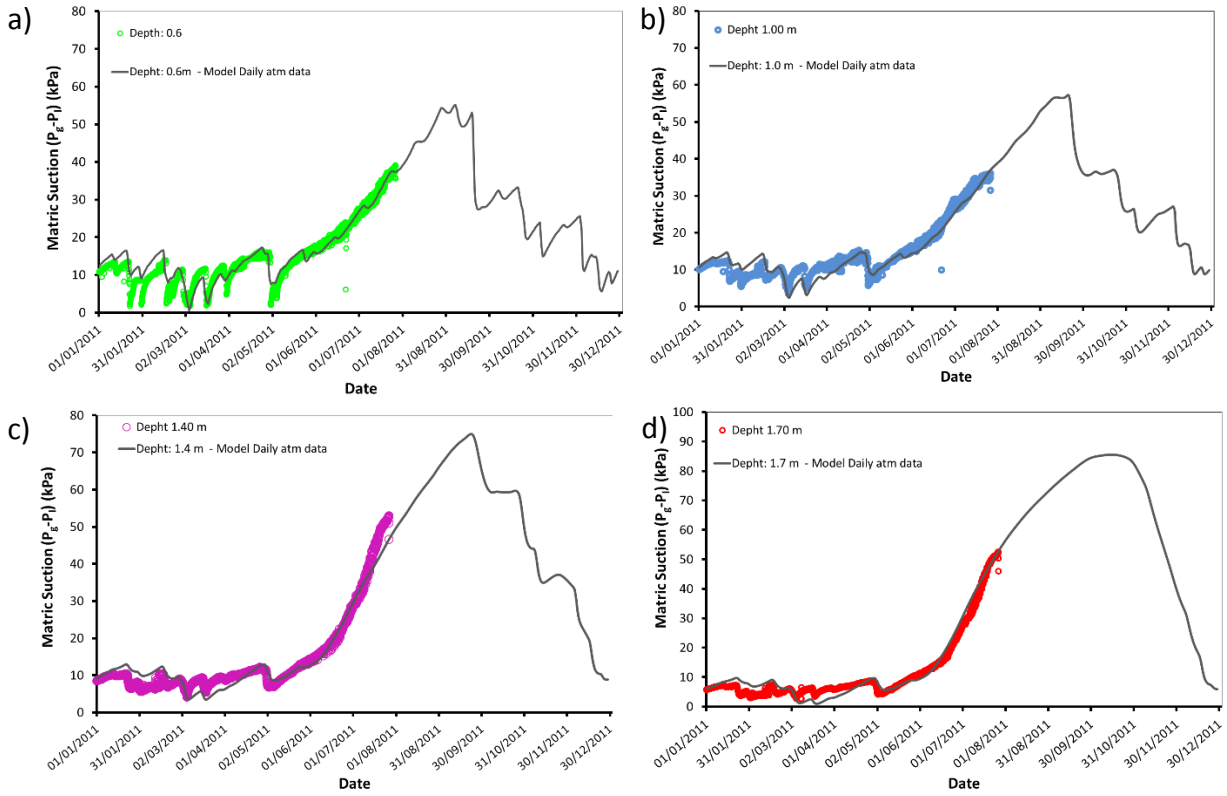

Figure 4-38 Liquid pressure evolution obtain for year 2011 a) 0.60 m depth b) 1.0 m depth c) 1.40 m depth d) 1.70 m depth

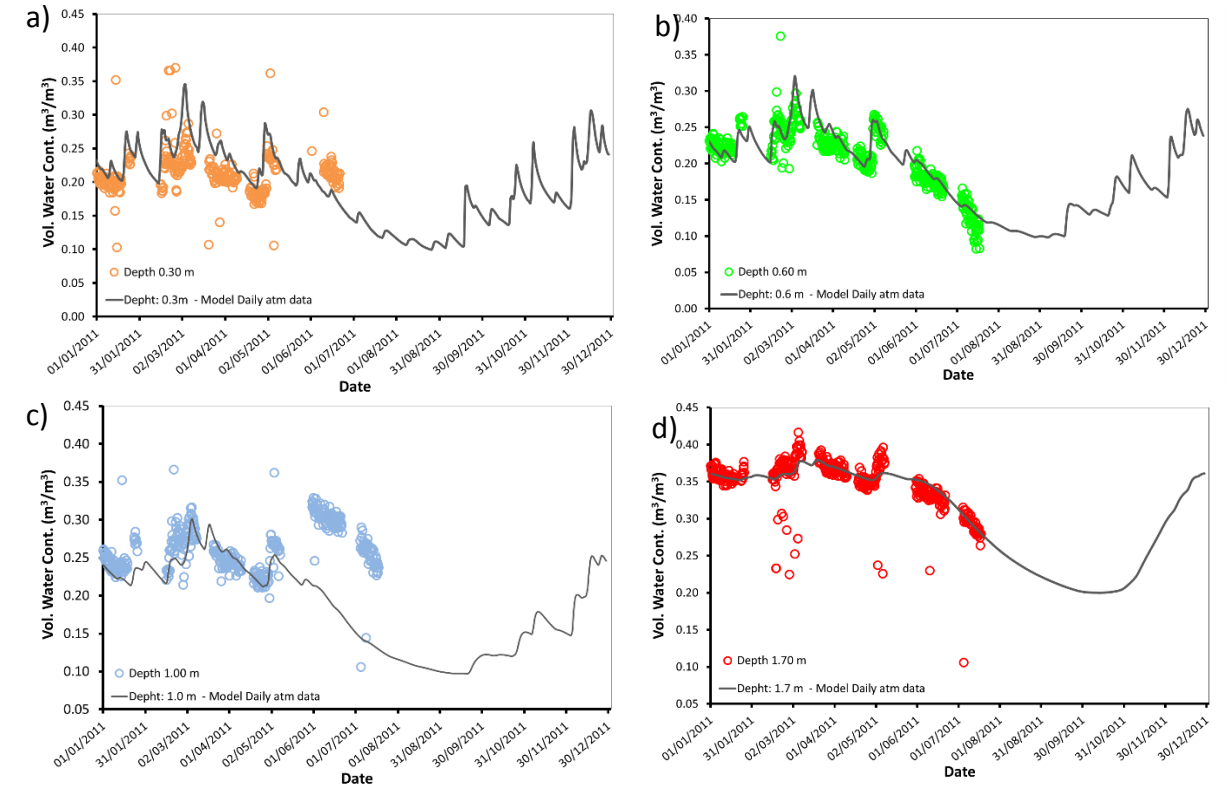

Figure 4-39 Volumetric water content evolution obtain for year 2011 a) 0.30 m depth b) 0.60 m depth c) 1.00 m depth d) 1.70 m depth

CHAPTER 5
CONCLUSIONS AND FUTURE WORK

5.1 CONCLUDING REMARKS

The region of Cervinara had been submitted in several occasions to rain-induced landslides. This zone is covered by unsaturated pyroclastic materials with a very high porosity. Which makes it very susceptible to collapse.This conditions coupled with the important inclination of the slope makes that the Cervinara pyroclastic soils very susceptible to failure caused by the decreasing in suction which leads to a reduction in shear strength.

The characteristics of this material had been evaluated at different scales: laboratory tests, slope scale and the real slope. The most important characteristic evidenced at all levels is that this material present a double porosity. This is to say, the material present an important quantity of pores with a size of intergranular pores but also a considerable quantify of intragranular pores. For this reason the implementation of a bimodal water retention curve had been very important to obtain adequately results at all the scales of analysis considered.

Even so, it is evidenced that hydraulic behaviour is influenced by the scale effect. In other words, the hydraulic characteristics of the material are different for the three scales study. on the other hand, the mechanical behaviour was properly defined by the response observed during by the test realize at the laboratory scale.

The flume test, is an interesting test that leads to evaluate the behaviour of the triggering of shallow landslides the model realized for this scale well reproduces the failure process observed with the test. But, for the cases of high porosity the response achieved do not reproduce the settlements due to collapse, although, it is able to well reproduce the failure moment and well evidenced the landslide failure.

On the other hand, the evolution of water content for this test was carried on with a new technique that allows to obtain the profile of water content installing just one TDR probe. It was observed that the profiles measured agree with the infiltration process expected for this type of test. The response achieved with the model, also present the trend expected, but present some discrepancy for the moment when failure is close.

Finally, for the real slope of Cervinara is observed that the hydraulic process that occurs within the soil corresponds to a response over a Thermo-hydraulic process as a reply of the atmospheric process that occurred at the interface ground-atmosphere. Additionally in this region the effect of the aquifer located in bedrock generates an important influence in the material above this effect can be represented by a boundary conditions that generates a suction ramp within the rock.

The evaporation and evapotranspiration fluxes present an important effect in the response achieved within the material. The back-analysis over these parameters appears to be an eminently suited strategy.

The prediction presented for test C4 was designated as winner of the benchmark on hydrological modelling slopes at the Italian Workshop on Landslides, 23rd October 2013.

5.2 FUTURE WORK

The failure of slopes triggered by rainfall is a complex phenomenon, as had been presented it involves a different types of process, hydraulic, thermal and mechanical, in order to improve the results presented and the analysis of the triggering process of this type of landslides, is important to consider the next lines:

- Improve the mechanical model implemented in the flume test, allowing to obtain the collapse settlements evidenced in the measures realized.
- Improve the effect of the vegetation in the slope response, and evaluate the effect of different roots depth.
- Consider the mechanical response of the real slope, in order to observe the settlements expected for the atmospheric climatic action. This response should be coupled with real data measures.
- Evaluate the effect of slope inclination on the results of the numerical model, consider the real geometry of the model, and evaluate the effect of the inclination in the response of liquid pressure.

REFERENCES

Alonso, E.E., Gens, A. & Josa, A., 1990. A constitutive model for partially saturated soils. *Géotechnique*, 40(3), pp.405–430.

Askarinejad, A. et al., 2011. Comparison between the in situ and laboratory water retention curves for a silty sand. *Unsaturated Soils-Proceedings of 5th international conference on unsaturated soils, sept 6-8 2010, Barcelona*, pp.423–428.

Askarinejad, A. et al., 2012. Unsaturated hydraulic conductivity of a silty sand with the instantaneous profile method. *Unsaturated Soils: Research and applications*, 2, pp.215–220.

Blight, G., 1997. Interactions between the atmosphere and the earth. *Geotechnique*, 47(4), pp.715–767.

Cascini, L., Cuomo, S. & Sorbino, G., 2005. Flow-like mass movements in pyroclastic soils: remarks on the modelling of triggering mechanisms. *Rivista italiana di geotecnica*, (4), pp.11–31.

Casini, F. et al., 2012. Consequences on water retention properties of double-porosity features in a compacted silt. *Acta Geotechnica*, 7(2), pp.139–150.

Comegna, L. et al., 2013. Effects of the Vegetation on the Hydrological Behavior of a Loose Pyroclastic Deposit. *Procedia Environmental Sciences*, 19, pp.922–931.

Damiano, E., Olivares, L. & Picarelli, L., 2012. Steep-slope monitoring in unsaturated pyroclastic soils. *Engineering Geology*, 137-138, pp.1–12.

Frost, J. & Park, J., 2003. A critical assessment of the moist tamping technique. *ASTM geotechnical testing journal*, 26(1), pp.1–14.

González, N., 2011. *Development of a family of constitutive models for geotechnical applications*.

Greco, R. et al., 2013. Hydrological modelling of a slope covered with shallow pyroclastic deposits from field monitoring data. *Hydrology and Earth System Sciences Discussions*, 10(5), pp.5799–5830.

Greco, R. et al., 2010. Soil water content and suction monitoring in model slopes for shallow flowslides early warning applications. *Physics and Chemistry of the Earth, Parts A/B/C*, 35(3-5), pp.127–136.

Greco, R., 2006. Soil water content inverse profiling from single TDR waveforms. *Journal of Hydrology*, 317(3-4), pp.325–339.

Leroueil, S., 2001. Natural slopes and cuts: movement and failure mechanisms. *Geotechnique*.

Noilhan, J. & Mahfouf, J.-F., 1996. The ISBA land surface parameterisation scheme. *Global and Planetary Change*, 13(1-4), pp.145–159.

Noilhan, J. & Planton, S., 1989. A simple parameterization of land surface processes for meteorological models. *Monthly Weather Review*, 17, pp.536–549.

Olivares, L. & Damiano, E., 2007. Postfailure Mechanics of Landslides: Laboratory Investigation of Flowslides in Pyroclastic Soils. *Journal of Geotechnical and Geoenvironmental Engineering*, 133(1), pp.51–62.

Olivares, L., Damiano, E. & Greco, R., 2009. An instrumented flume to investigate the mechanics of rainfall-induced landslides in unsaturated granular soils. *ASTM geotechnical testing Journal.*, 32(2).

Olivares, L. & Tommasi, P., 2008. The role of suction and its changes on stability of steep slopes in unsaturated granular soils. *Landslides and Engineered Slopes. From the Past to the Future*, pp.203–215.

Olivella, S. et al., 1994. Nonisothermal multiphase flow of brine and gas through saline media. *Transport in porous media*.

Olivella, S. et al., 1996. Numerical formulation for a simulator (CODE_BRIGHT) for the coupled analysis of saline media. *Engineering Computations*, 13(7), pp.87–112.

Penman, H.L., 1948. Natural evaporation from open water, hare soil and grass. *Proceedings of the Royal Society of London. Series A: Mathematical and physical sciences*, 193(1032), pp.120–145.

Picarelli, L. & Vinale, F., 2007. AMRA: laboratory equipment. *Report-Centro Euro-Mediterraneo per i cambiamenti climatici*.

Rahardjo, H. & Lee, T., 2005. Response of a residual soil slope to rainfall. *Canadian Geotechnical Journal*, 42(2), pp.340–351.

Rahardjo, H., Satyanaga, A. & Leong, E., 2011. Unsaturated soil mechanics for slope stabilization. *Unsaturated soils: Theory and practice …*, pp.103–117.

Rianna, G., Pagano, L. & Urciuoli, G., 2014. Rainfall patterns triggering shallow flowslides in pyroclastic soils. *Engineering Geology*, 174, pp.22–35.

Saaltink, M., Pereira, J. & Samat, S., 2011. Atmospheric boundary conditions module in CODE_BRIGHT.

Sellers, P.J. et al., 1986. A simple biosphere model (SiB) for use within general circulation models. *Journal of the the atmospheric sciences*, pp.505 – 531.

Springman, S. & Askarinejad, A., 2012. Lessons learnt from field tests in some potentially unstable slopes in Switzerland. *Acta Geotechnica slovenica*, 1, pp.5–29.

Vaunat, J. et al., 2012. Slope responses under climatic actions. Model and case interpretation. *In preparation*.

WeatherSpark, 2014. Average Weather For Naples, Italy - WeatherSpark. Disponible en http://weatherspark.com/#!dashboard;q=Naples%20NA%2C%20Italy

Yu, H.S., 1998. CASM: a unified state parameter model for clay and sand. *International Journal for Numerical and Analytical Methods in Geomechanics*, 22(8), pp.621–653.